NAVAL AIR WARFARE CENTER AIRCRAFT DIVISION
PATUXENT RIVER, MARYLAND

TECHNICAL MEMORANDUM

REPORT NO: NAWCADPAX--98-225-TM

STATIC AND DYNAMIC CHARACTERIZATION
OF HELMET TRACKERS

11 March 1999

Approved for public release; distribution is unlimited.

DTIC QUALITY INSPECTED 4

19990820 078

DEPARTMENT OF THE NAVY
NAVAL AIR WARFARE CENTER AIRCRAFT DIVISION
PATUXENT RIVER, MARYLAND

NAWCADPAX--98-225-TM
11 March 1999

PREPARED BY:

Joseph Hamilton   11 MAR '99

JOSEPH HAMILTON / DATE

RELEASED BY:

Richard Dunn   11 MAR '99

RICHARD S. DUNN, Ph.D. / DATE
Head, Crewstation Technology Laboratory
Naval Air Warfare Center Aircraft Division

Chris Grable   3-11-99

CHRIS GRABLE / DATE
Head, Human Engineering Applications Branch
Naval Air Warfare Center Aircraft Division

REPORT DOCUMENTATION PAGE		Form Approved OMB No. 0704-0188
Public reporting burden for this collection of information is estimated to average 1 hour per response, including the time for reviewing instructions, searching existing data sources, gathering and maintaining the data needed, and completing and reviewing the collection of information. Send comments regarding this burden estimate only, other aspect of this collection of information, including suggestions for reducing this burden, to Washington Headquarters Services, Directorate for Information Operations and Reports, 1215 Jefferson Davis Highway, Suite 1204, Arlington, VA 22202-4302, and to the Office of Management and Budget, Paperwork Reduction Project (07804-0188), Washington, DC 20503.		
1. AGENCY USE ONLY *(LEAVE BLANK)*	2. REPORT DATE 11 March 1999	3. REPORT TYPE AND DATES COVERED
4. TITLE AND SUBTITLE Static and Dynamic Characterization of Helmet Trackers		5. FUNDING NUMBERS
6. AUTHOR(S) Joseph Hamilton (NASA Johnson Space Center/SP2)		
7. PERFORMING ORGANIZATION NAME(S) AND ADDRESS(ES) Naval Air Warfare Center Aircraft Division 22347 Cedar Point Road, Unit #6 Patuxent River, Maryland 20670-1161		8. PERFORMING ORGANIZATION REPORT NUMBER NAWCADPAX--98-225-TM
9. SPONSORING/MONITORING AGENCY NAME(S) AND ADDRESS(ES) Naval Air Warfare Center Aircraft Division 4.6 Crew Systems Division, Bldg. 2187 48110 Shaw Road, Unit #5 Patuxent River, Maryland 20670-1906		10. SPONSORING/MONITORING AGENCY REPORT NUMBER
11. SUPPLEMENTARY NOTES Significant contributions to this project and report were made by several members of the Crewstation Technology Laboratory team including: Richard S. Dunn, Ph.D. Donna L. Culver LT Edward Bachelder, USNR Mike Howell Wayne Erchak Chris Bolden W. Patrick Gatewood RM-1 Dave Westfall, USN		
12a. DISTRIBUTION/AVAILABILITY STATEMENT Approved for public release; distribution is unlimited.		12b. DISTRIBUTION CODE
13. ABSTRACT *(Maximum 200 words)* This report documents a project to develop an independent government capability to assess the performance and limitations of commercially manufactured helmet trackers. The Polhemus 3Space FASTRAK® and the Ascension Flock of Birds® helmet trackers were evaluated and the results are included in this report. The test equipment and methods developed for this project will be used to evaluate newer systems as helmet tracker technology continues to improve.		

This report documents a project to develop an independent government capability to assess the performance and limitations of commercially manufactured helmet trackers. The Polhemus 3Space FASTRAK® and the Ascension Flock of Birds® helmet trackers were evaluated and the results are included in this report. The test equipment and methods developed for this project will be used to evaluate newer systems as helmet tracker technology continues to improve.

14. SUBJECT TERMS		15. NUMBER OF PAGES
Helmet Mounted Display (HMD) Helmet Trackers FASTRAK® Flock of Birds®		68
		16. PRICE CODE

17. SECURITY CLASSIFICATION OF REPORT	18. SECURITY CLASSIFICATION OF THIS PAGE	19. SECURITY CLASSIFICATION OF ABSTRACT	20. LIMITATION OF ABSTRACT
Unclassified	Unclassified	Unclassified	SAR

SUMMARY

This report documents a project to develop an independent government capability to assess the performance and limitations of commercially manufactured helmet trackers. The Polhemus 3Space FASTRAK® and the Ascension Flock of Birds® (FOB) helmet trackers were evaluated and the results are included in this report. The test equipment and methods developed for this project will be used to evaluate newer systems as helmet tracker technology continues to improve.

The test equipment consisted of a wooden table with nonmetallic fittings to allow multiple test configurations and a motor on a separate table driving a nonmetallic rod in a sinusoidal motion for dynamic tests. An SGI Indigo2 computer recorded the data from the tracker and from a sensor indicating the actual rod position. Noise and error sources were reduced as practical, but not eliminated.

The FASTRAK® was evaluated in a typical configuration with optional filters off. The FOB was evaluated with selectable filters on and off. The trackers were tested statically for accuracy and precision, but most of the project emphasis was on dynamic accuracy with three different types of motion (translation only, rotation only, and combined translation and rotation). Dynamic tests were conducted with a fixed configuration at multiple frequencies as well as at a fixed frequency with multiple configurations. Significant findings are documented in this report and selected plots of the data are included in the appendices.

Both trackers showed good static precision that decayed with distance between the transmitter and the receiver. The filters on the FOB greatly increased the static precision. Significant static errors, particularly when an error source was close to the receiver, were measured for both trackers. The errors were repeatable in a given environment indicating that a method of mapping the environment could reduce static error to acceptable levels.

Dynamic results were more complicated. Static error appeared as a component of dynamic error. Latency caused dynamic errors that increase with velocity due to the difference between where the receiver was when the sample was taken, and where the receiver was when the sample was reported. Other errors occurred when a moving receiver read a different value than the static value at the same position and orientation. This may have been caused by moving electric coils in a magnetic field, software filters, or other factors unique to the design of the tracker. Both trackers showed errors that depend upon the magnitude and direction of the receiver velocity relative to the transmitter, as well as the location of the receiver relative to the transmitter. Generally, dynamic error increased when the receiver was moved closer to transmitter. Dynamic error was repeatable in a given environment and could potentially be reduced by compensating for the position and velocity of the receiver relative to the transmitter.

Both trackers contained a sweet spot where the combination of static and dynamic errors could be minimized. Smart filters might further reduce the errors by considering the position and velocity of the receiver relative to the transmitter. Testing of a tracker in various configurations may identify the best settings to use to obtain desired performance for a particular job.

CONTENTS

INTRODUCTION

1.   All types of visually coupled systems, including helmet-mounted displays (HMD's) depend upon some type of head position tracker to direct a computer or sensor (or both). In combination with task and operator factors, helmet trackers can constrain or limit HMD system performance. Thus, selecting and programming the tracker is a key aspect of HMD system design and development.

2.   Information concerning helmet tracker performance is not generally available to HMD system developers and testers. Available data on accuracy, precision, and jitter concerns mainly static performance. NAWCAD Patuxent River, Crewstation Technology Laboratory (CTL), has long sought a practical means to test and demonstrate dynamic helmet tracker performance.

3.   The achievement of that goal, as shown in this report, can lead to effective discriminations between helmet tracker systems, assessments of task dependent system performance issues and establishment of clear performance requirements for military system helmet trackers. The new capability to assess helmet tracker dynamic performance can also help to guide helmet tracker technology investment in terms of which technical approaches to develop, what refinements to emphasize for best performance, and how advanced software may be able to compensate for basic limitations in dynamic performance. This report concerns magnetic helmet trackers but the techniques discussed can also be applied to the other basic types including acoustic, optical, mechanical, and inertial.

BACKGROUND

4.   The CTL applied available internal resources to develop a methodology for testing helmet tracker devices. Each device has unique capabilities and limitations. Environmental conditions may effect one type of tracker significantly while having little or no effect on a different tracker that uses different technology. Prior testing confirmed that operations using a helmet tracking system can be very sensitive to error (reference 1). The ability to characterize the performance and susceptibility to error of various trackers will be valuable to all government organizations that are interested in helmet tracker technology.

5.   The approach taken to develop a methodology for testing helmet tracker devices was to use available trackers and computers and to create an inexpensive prototype test environment. The test equipment and software were modified as the results of early testing helped to identify areas of improvement.

6.   The static performance of helmet trackers is easily understood and relatively well known. Previous dynamic testing of helmet trackers attempted to measure the latency by observing the phase lag of the output given a sinusoidal input. Latency will cause dynamic errors that increase with velocity due to the difference between where the receiver was when the sample was taken, and where the receiver was when the sample was reported. Unfortunately, a wide range of latencies were reported depending upon the method used. One team even reported a negative latency (reference 2). One difficulty in this method is the assumption that the output is also

sinusoidal. Distortions in the shape of the output can occur. Static error appears as a component of dynamic error. Other errors can occur when a moving receiver reads a different value than the static value at the same position and orientation. This may be caused by moving electric coils in a magnetic field, software filters, or other factors unique to the design of the tracker.

7.   Emphasis on developing methods to identify and characterize dynamic error is required to describe the performance of helmet trackers for typical use. Dynamic errors can depend upon the magnitude and direction of the receiver velocity relative to the transmitter, as well as the location of the receiver relative to the transmitter. Various methods of visually presenting the output were explored and have provided some unique insights into the performance of the trackers.

PURPOSE

8.   The purpose of this report is to document a project to develop an independent government capability to assess the performance and limitations of commercially manufactured helmet trackers.

DESCRIPTION OF TEST EQUIPMENT AND SOFTWARE

9.   The test equipment consisted of the following:

   a.   A wooden table with nonmetallic fittings to allow multiple test configurations (see figure 1).

   b.   A motor on a separate table driving a nonmetallic rod in a sinusoidal motion for dynamic tests (see figure 1).

   c.   An analog sensor (linear resistor) indicating the actual rod position as voltage to an analog-to-digital (A/D) converter.

   d.   An SGI Indigo2 computer for recording the data from the tracker and the analog sensor.

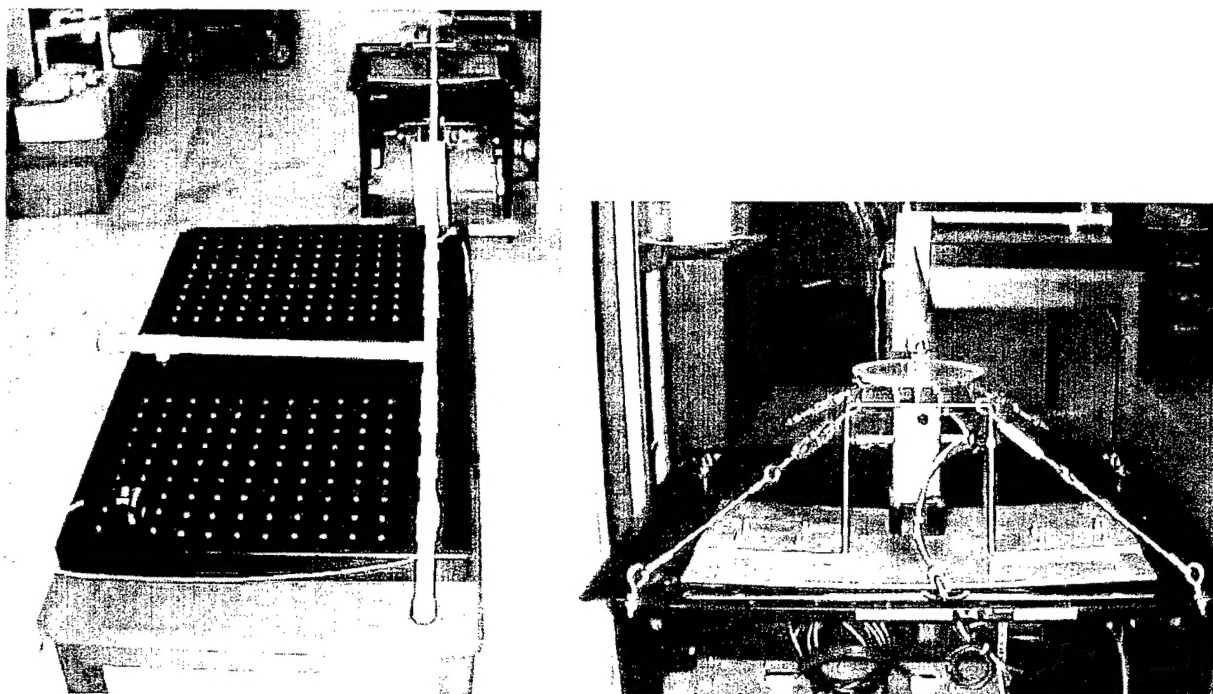   e.   A helmet tracker (see Description of Test Articles).

Figure 1
TEST AND MOTOR TABLES

10. Custom test equipment was developed for this project using nonmetallic fasteners and adhesives. The wooden test platform with a grid of fixture placement holes spaced on 2-in. centers supported multiple testing configurations using plastic mounting plates for the helmet tracker components. The platform was attached to a wooden table. The moving element of the apparatus was constructed of common plastic plumbing pipe by machining the inside of t-fixtures for a smooth sliding fit. The jointed assembly allowed placement of helmet tracker components in selected positions to achieve linear, rotary, or both motions simultaneously. The moving assembly was driven by a variable speed electric motor mounted on a separate stand. The motor table was moved far enough away from the test table so that the static output of the tracker was not measurably effected by the presence of the motor table. Tests were conducted in the middle of a laboratory room on a concrete floor. Noise and error sources were reduced as practical, but not eliminated. A connecting rod with two selectable crank offsets converted the motor's rotary motion to sinusoidal movement in the helmet tracker test stand. Overall linear motion amplitude was 2 or 4 in. Working speed of the unit provided up to 10 Hz at the smaller amplitude and up to 5 Hz at the larger.

11. A linear resistor was connected to sense the sliding rod position. This signal was converted in a dedicated high-speed A/D circuit. The tracker and the A/D converter were connected to the SGI via RS-232 serial ports at 38400 baud. The minimum resolution of the resistor was 0.0034 in. or 0.17% of the 2-in. linear motion.

12. The software on the SGI was written in C++ to read the tracker being tested in continuous or stream mode. This resulted in 120 unique samples per second for the FASTRAK® and 316 nonunique samples per second for the Flock of Birds® (FOB). The FOB updated about 103 times a second so every third or fourth sample provided new data. In addition to the C++ program, a small Basic/Assembly language program was loaded on the control card for the A/D converter to tell it the format and content of the serial communications. Upon receipt of a sample from the tracker, the software would poll the A/D converter and record the data with a time stamp. The A/D converter was extremely fast relative to the trackers tested and significant effort was made to receive and record the data with minimal delay. The latency between receiving a tracker sample and attaching an analog value to it was between 0.27 and 0.36 msec. The minimum latency includes 0.26 msec to send a 1 byte poll command at 38,400 baud and 0.01 msec for the converter to sample the resistor. The maximum latency was measured on an oscilloscope from the start of the poll command to the start of the return message.

DESCRIPTION OF TEST ARTICLES

13. Two helmet trackers were used for this project. Both were available systems in general use at the CTL. The first was a lab grade 3-Space FASTRAK® system supplied in 1993 by Polhemus, Inc., (Model 3SF0002, S/N 1330252). The system has been employed in numerous CTL tests, simulations and trials, and operates dependably. The second unit was a FOB device supplied in 1997 by Ascension Technology, Corporation (Model 6DFOB, S/N 003326). This product was recently acquired and has only been operated for informal testing. Both trackers were designed to mount a receiver to the helmet of an aircrew member. The exact technology varies with each tracker, but both systems transmit a reference magnetic field. A receiver reads the position and orientation of the helmet with respect to the reference transmitter. Multiple receivers can be connected to the signal processing unit for both systems, but only the single receiver configuration was tested. The output was provided digitally in selectable formats on an RS-232 serial port. Figures 2 and 3 map the timelines for data collection in the test configuration. The FOB timeline is shorter because FOB sent a 12 byte message instead of 29 bytes for the FASTRAK®.
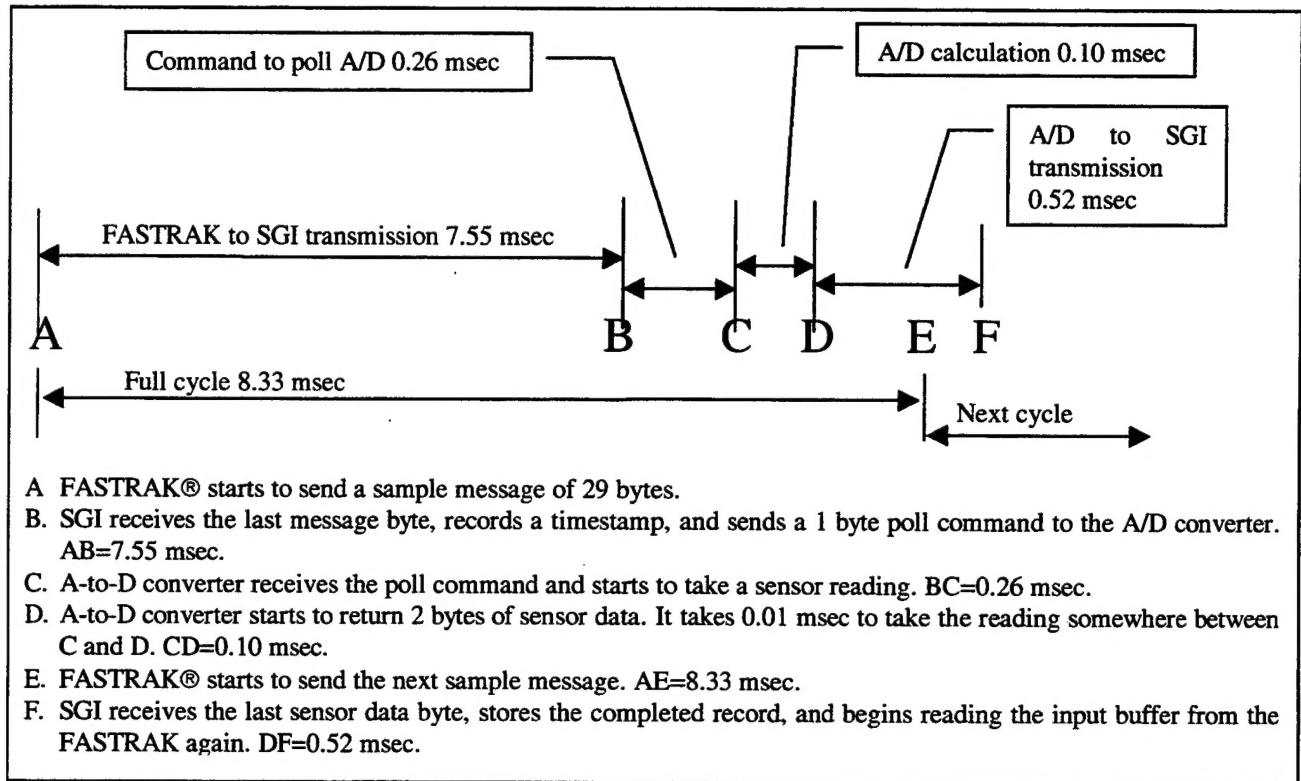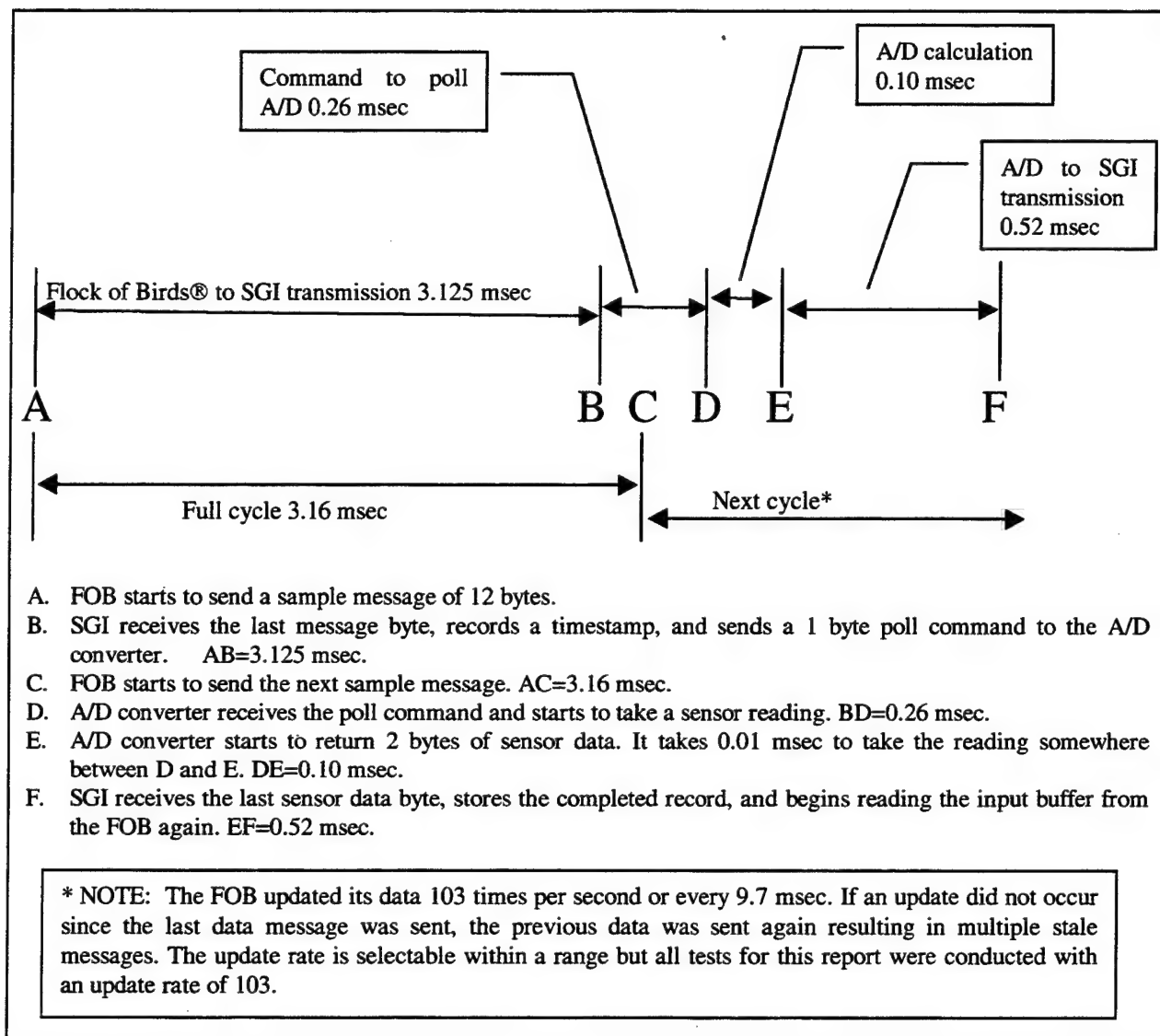
Figure 2
FASTRAK® LATENCY TIMELINE

The content of Figure 2 is as follows:

Command to poll A/D 0.26 msec

A/D calculation 0.10 msec

A/D to SGI transmission 0.52 msec

FASTRAK to SGI transmission 7.55 msec

A   B   C   D   E F

Full cycle 8.33 msec   Next cycle

A FASTRAK® starts to send a sample message of 29 bytes.
B. SGI receives the last message byte, records a timestamp, and sends a 1 byte poll command to the A/D converter. AB=7.55 msec.
C. A-to-D converter receives the poll command and starts to take a sensor reading. BC=0.26 msec.
D. A-to-D converter starts to return 2 bytes of sensor data. It takes 0.01 msec to take the reading somewhere between C and D. CD=0.10 msec.
E. FASTRAK® starts to send the next sample message. AE=8.33 msec.
F. SGI receives the last sensor data byte, stores the completed record, and begins reading the input buffer from the FASTRAK again. DF=0.52 msec.

Figure 3
FOB LATENCY TIMELINE

The diagram contains the following labeled elements:

- Command to poll A/D 0.26 msec
- A/D calculation 0.10 msec
- A/D to SGI transmission 0.52 msec
- Flock of Birds® to SGI transmission 3.125 msec
- A, B, C, D, E, F (timeline points)
- Full cycle 3.16 msec
- Next cycle*

A. FOB starts to send a sample message of 12 bytes.
B. SGI receives the last message byte, records a timestamp, and sends a 1 byte poll command to the A/D converter.   AB=3.125 msec.
C. FOB starts to send the next sample message. AC=3.16 msec.
D. A/D converter receives the poll command and starts to take a sensor reading. BD=0.26 msec.
E. A/D converter starts to return 2 bytes of sensor data. It takes 0.01 msec to take the reading somewhere between D and E. DE=0.10 msec.
F. SGI receives the last sensor data byte, stores the completed record, and begins reading the input buffer from the FOB again. EF=0.52 msec.

> * NOTE: The FOB updated its data 103 times per second or every 9.7 msec. If an update did not occur since the last data message was sent, the previous data was sent again resulting in multiple stale messages. The update rate is selectable within a range but all tests for this report were conducted with an update rate of 103.

SCOPE OF TESTS

14. The tests were conducted one at a time in a laboratory environment. For each test, the tracker was attached to a dedicated test computer. No other functions (like display generation) were conducted or tested.

15. The trackers were tested statically for accuracy and precision and dynamically for accuracy with three different types of motion: translation only, rotation only, and combined translation and rotation.

16. Static testing was conducted to characterize nominal static performance and to subjectively analyze interactions between the tracker and typical cockpit or laboratory items that might interfere with tracker performance. Exact formal mapping of the static error in the laboratory environment was not attempted.

17. Dynamic tests were conducted with three different types of motion: motion in translation, motion in rotation, and combined motion in translation and rotation simultaneously. For each type of motion, two tests were conducted. One test involved a fixed transmitter orientation and location while the receiver was moved in a sinusoid at multiple frequencies. Frequencies ranged from 1 to 10 Hz. The other dynamic tests were conducted at a fixed frequency with multiple transmitter locations.

18. Many different configurations and orientations are possible for each tracker. For this report, the FASTRAK® was evaluated in a typical configuration with optional filters off. The results are captured in appendix A. The FOB was evaluated in two different configurations with the results captured in appendices B (default filters on) and C (selectable filters off).

METHOD OF TESTS

19. The static test was performed by attaching the transmitter to one side of the table and placing the receiver at different points along a marked line. The marks were at 1-in. increments and ranged from 3 to 43 in. from the center of the transmitter. The receiver was attached to a plastic ruler to help keep the orientation correctly aligned at each point. Minor deviations in azimuth are possible with this method due to human error in aligning the ruler, but roll and elevation should be accurate. If it is important to accurately measure all three angles, a second test with a different orientation can be conducted, or a simple slide mechanism could be built. A 1/2 sec of data was recorded at each point on the line.

20. Dynamic tests were conducted by attaching the drive rod to the motor disk at a radius from the center of the disk to establish the amplitude of the sinusoidal motion. Higher frequencies were possible at lower amplitude. A radius of 1 in. was selected for these tests to provide frequencies up to 10 Hz. The tracker receiver was placed at one of three locations. The first location is on the rod to provide a linear translation of 2 in. The second location was at the pivot point of the cross bar to provide angular rotation of .087 radians. The third location was on the cross bar, near the rod, to provide combined motion with translation and rotation components. For each receiver location, two tests were conducted. The slow frequency test involved setting the motor speed to approximately 1.6 Hz and recording samples while the transmitter was moved from close to far away from the receiver. The second test involved placing the transmitter at a middle distance and recording samples at different frequencies.

DATA ANALYSIS

21. Data were plotted and analyzed using available mathematical software packages.

22. Static precision was determined by calculating the root mean square (RMS) of many data samples taken from the static location. The RMS was plotted against the range as reported by the tracker. This worked well with the exception that the Flock of Birds® settings used for the test inhibited reporting of distances beyond 36 in. on an axis. Static accuracy was determined by comparing the mean output to the visually measured distance and orientation.

23. Dynamic tests were analyzed by several methods. Visual inspection of the raw data confirmed the integrity of the data. By calculating a gain and phase angle at different frequencies, Bode plot information was obtained. A computer simulation of the test setup with selectable latency was developed to provide a basis for comparison. The difference between the actual and simulated outputs helped to isolate nonlatency-related dynamic errors. The simulation could be expanded in future tests to model nonlatency errors. This model could be used to predict the output of the tracker for any position and orientation given a specified configuration. This would be a first step towards designing a smart filter to. compensate for selected errors during operational use.

24. Color plots of the outputs versus time showed deviations from the expected sinusoidal output. Color plots of the tracker output versus the "truth sensor" at multiple frequencies and in multiple configurations provided significant insight into the pattern of error sources.

DISCUSSION

GENERAL

25. The results from both trackers showed good static precision that decayed with distance between the transmitter and the receiver. Significant static errors, particularly when an error source was close to the receiver, were measured for both trackers. The errors were repeatable in a given environment indicating that a method of mapping the environment could reduce static error to acceptable levels. Generally, dynamic error increased when the receiver was moved closer to the transmitter. Dynamic error was repeatable in a given environment and could potentially be reduced by compensating for position and velocity of the receiver relative to the transmitter.

STATIC PRECISION

26. Static precision was significantly improved for the FOB tracker with the filters on (see figures B1.1, B1.2, C1.1, and C1.2). Static precision for the FASTRAK® was good without filters. FASTRAK® performance with the filters on was not tested.

STATIC ACCURACY

27. The FASTRAK® appeared to be more susceptible to disturbance from metal in the vicinity than the FOB. Both trackers showed measurable errors when a CRT was placed in close proximity to the receiver. All output parameters for the FASTRAK® changed noticeably when the transmitter was placed at different distances from the receiver along a single axis without changing the relative orientation. The deviations were repeatable indicating that a thorough mapping of the environment could be used to compensate for the static errors if the environment does not change.

DYNAMIC ACCURACY

28. For both trackers, the location of the receiver relative to the transmitter had significant effects on the results. The dynamic error generally became larger as the receiver was moved closer to the transmitter. This effect was overshadowed by noise in the FOB with the filters turned off (The noise, at a distance, was greater than the dynamic error in close). The dynamic error showed up in several parameters at once, not just the stimulated parameter. The dynamic error increased as the frequency increased. Both trackers showed significant deviations from a sinusoidal output (with sinusoidal input). The most dramatic departure from sinusoidal motion came from the FOB with the filters on.

29. Appendices A, B, and C contain selected plots of output parameters versus time and output parameters versus the input to demonstrate the nature and magnitude of the dynamic errors measured. The combination of errors in multiple parameters created a complex picture of motion that is challenging to predict. However, the results of this testing indicate that it could be possible to reduce dynamic error in critical parameters for the task of following a moving target by considering the position and velocity vectors of the receiver relative to the transmitter.

DYNAMIC FREQUENCY RESPONSE

30. Latency was difficult to determine due to the nonsinusoidal nature of the output. However, latency measurements at frequencies above 3 Hz showed good consistency. The likely reason for this is that the error due to latency became the dominant source of error as phase lag increased. Gain for stimulated parameters remained approximately constant as frequency increased except in the FOB case with default filters on. Table 1 and figure 4 are examples of the frequency response results.

Table 1

GAIN, PHASE LAG, AND LATENCY OF FASTRAK® AND
FOB TRACKER SYSTEMS FOR MOVEMENT RATES UP TO 10 Hz

FASTRAK® Translate only (red lines in figure 4)

Frequency (Hz)	1.54	2.54	3.59	5.44	6.79	9.24
Gain	1.0149	1.0133	1.0154	1.0171	1.0207	1.0205
Phase lag (deg)	11	9	13	20	26	35
Latency (sec)	0.0198	0.0098	0.0101	0.0102	0.0106	0.0105

FOB Default Translate only (green lines in figure 4)

Frequency (Hz)	1.59	2.69	3.29	4.19	5.09	6.29	9.89
Gain	0.9965	0.9965	0.9888	0.9703	0.9487	0.9261	0.8077
Phase lag (deg)	27	39	58	73	89	110	161
Latency (sec)	0.0472	0.0403	0.0490	0.0484	0.0486	0.0486	0.0452

FOB (filters off) Translate only (blue lines in figure 4)

Frequency (Hz)	1.65	2.30	3.80	5.80	6.85	7.25
Gain	1.0235	1.0179	1.0226	1.0213	1.0246	1.0205
Phase lag (deg)	12	17	29	43	50	54
Latency (sec)	0.0202	0.0205	0.0212	0.0206	0.0203	0.0207
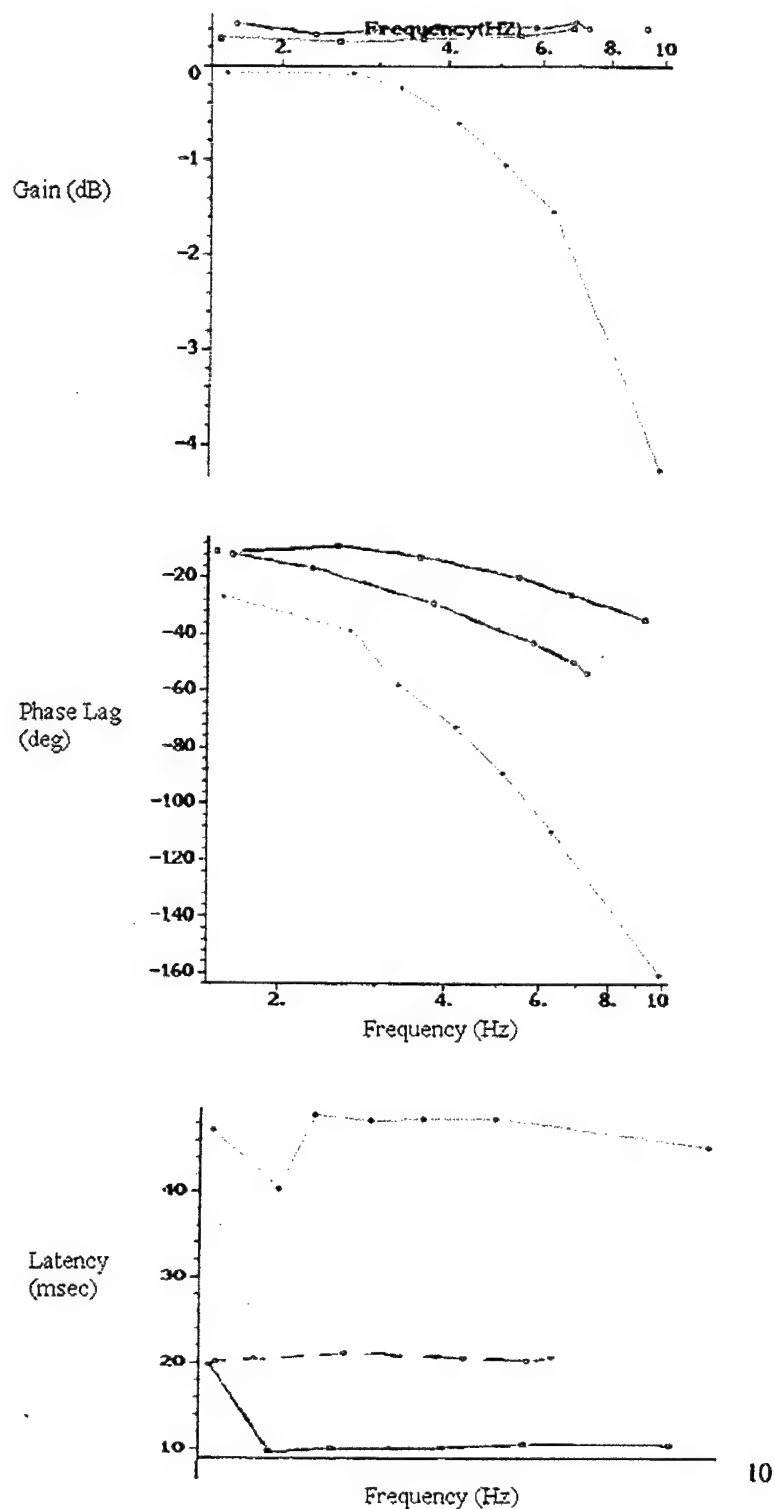
Figure 4
GAIN, PHASE LAG, AND LATENCY OF FASTRAK® AND
FOB TRACKER SYSTEMS FOR MOVEMENT RATES UP TO 10 Hz

11

THIS PAGE INTENTIONALLY LEFT BLANK

CONCLUSIONS

31. The CTL succeeded in its goal to develop a practical means to test and demonstrate static and dynamic helmet tracker performance.

32. Latency was measurable for each parameter of each tracker under test.

33. The output of both trackers showed deviations from sinusoidal motion that cannot be attributed to latency.

34. The output of both trackers showed measurable cross-coupled motion in parameters other than the ones stimulated (e.g., orientation and position output changed when only position was moved).

35. The filters on the FOB greatly reduced the static noise of the tracker, however, the filters had significant adverse effects on the dynamic performance of the tracker.

36. By testing different combinations of filter settings on the FOB, it is likely that a reasonable compromise between static precision and dynamic performance could be found for most applications.

37. Both trackers contained a sweet spot where the combination of static and dynamic errors could be minimized.

38. Smart filters might improve the performance of visual systems that use helmet trackers by compensating for selected dynamic errors as a function of the position and velocity of the receiver relative to the transmitter.

RECOMMENDATIONS

39. The CTL should apply the capability to assess helmet tracker dynamic performance to other basic types of trackers including acoustic, optical, mechanical, and inertial (paragraph 3).

40. The CTL should investigate the operational consequences of the dynamic and cross-coupled errors identified in this report.

41. The CTL should investigate the possibility of defining a smart filter that can improve the dynamic performance of helmet trackers.

42. The CTL should apply the lessons from this project to develop a capability to assess the dynamic performance of avionics grade trackers in the cockpit environment.

THIS PAGE INTENTIONALLY LEFT BLANK

REFERENCES

1. NAWCAD Patuxent River Technical Memorandum No. NAWCADPAX--96-173-TM, Air-to-Air Missile Firing Task Using a Helmet Mounted Display, of 15 July 1996.

2. Adelstein, B. D., Johnston, E. R., and Ellis, S. R.(1996), "Dynamic Response of Electromagnetic Spatial Displacement Trackers," Presence Volume 6, Number 3.

THIS PAGE INTENTIONALLY LEFT BLANK

APPENDIX A
FASTRAK® TESTS

Configuration:
Single transmitter
Single receiver
120 samples per second
Optional filters off.
RS-232 connection at 38,400 baud.

Description: The root mean square (RMS) of the noise in position parameters as a function of distance between the transmitter and the receiver as measured along the X axis by the tracker. The lowest line (red) is the noise in the X axis. The middle line (green) is the noise in the Y axis and the top line (blue) is the noise in the Z axis.
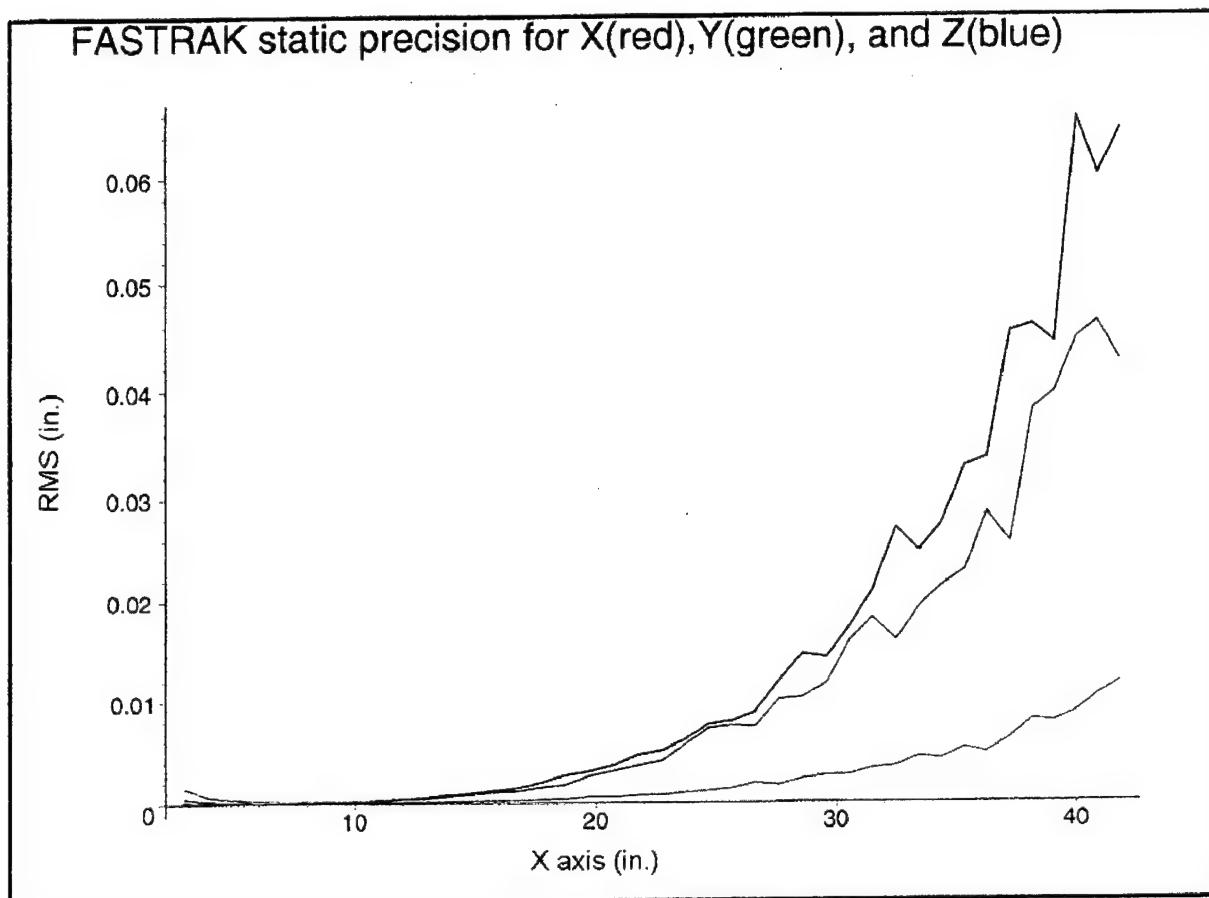
Figure A1.1
FASTRAK® STATIC PRECISION IN POSITION

Description: The RMS of the noise in orientation parameters as a function of distance between the transmitter and the receiver as measured along the X axis by the tracker. The top line (red) is the noise in azimuth. The middle line (green) is the noise in elevation and the lowest line (blue) is the noise in roll.
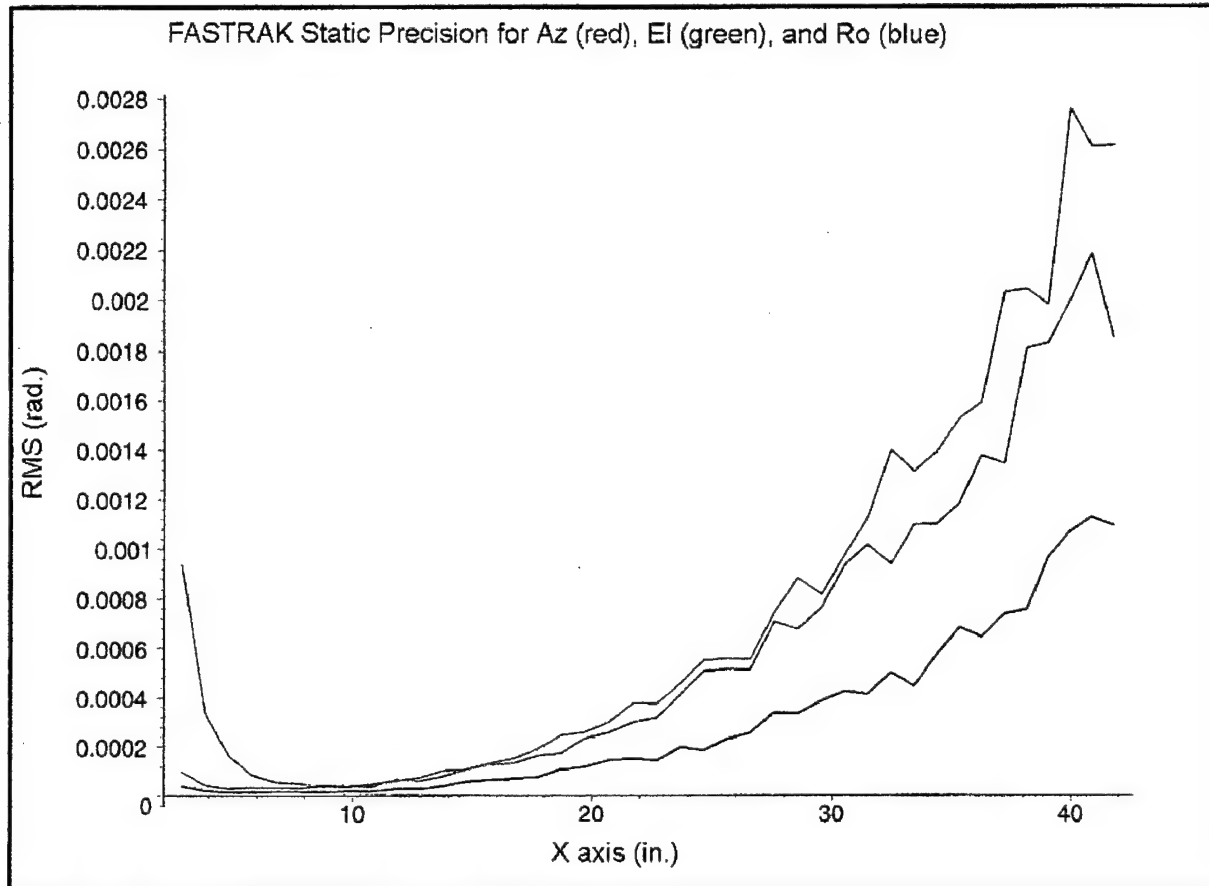
Figure A1.2
FASTRAK® STATIC PRECISION IN ORIENTATION

Description: The FASTRAK® X axis (red) and the analog sensor (black) versus time. The input movement is sinusoidal translation along the X axis at 1.6 Hz with 1 in. of amplitude. Parts of the curve match the input almost exactly while other parts show noticeable lag.
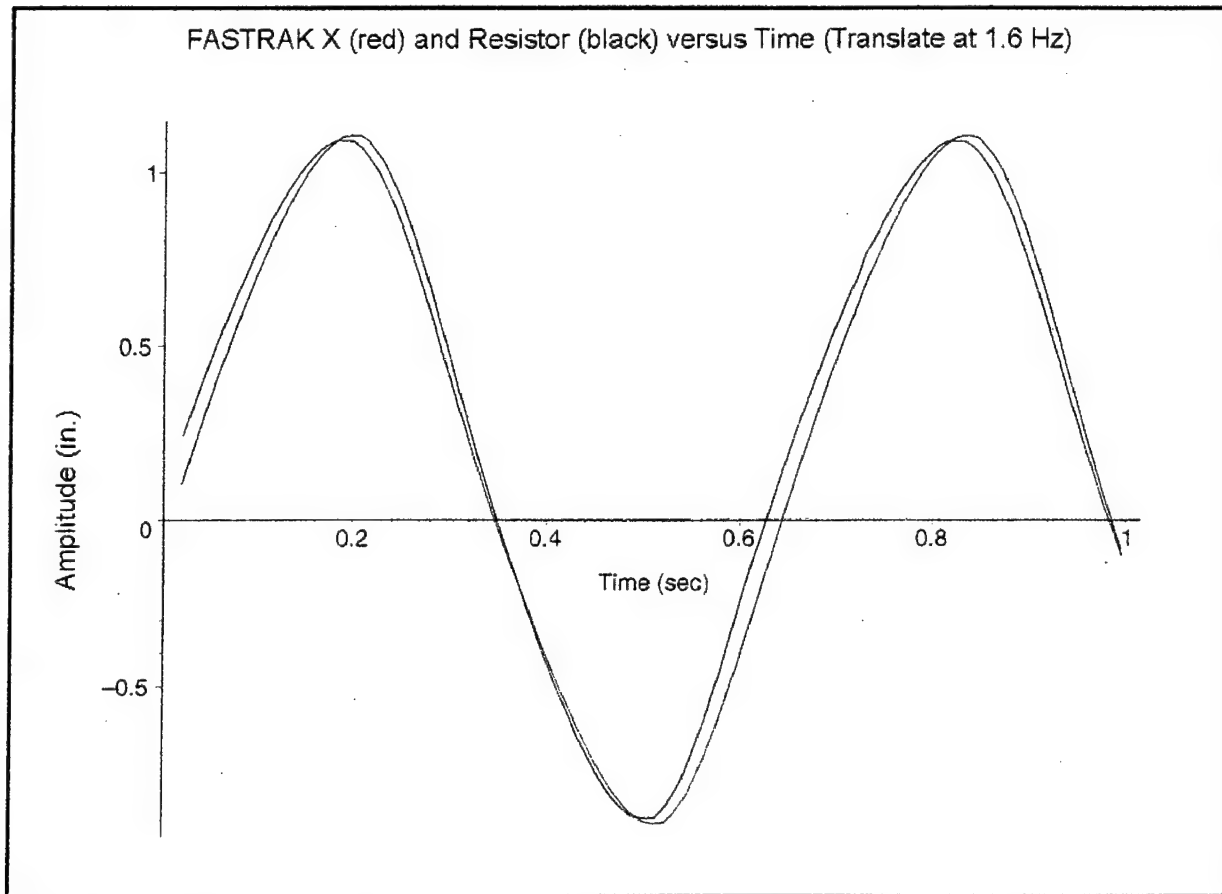
Figure A2.1
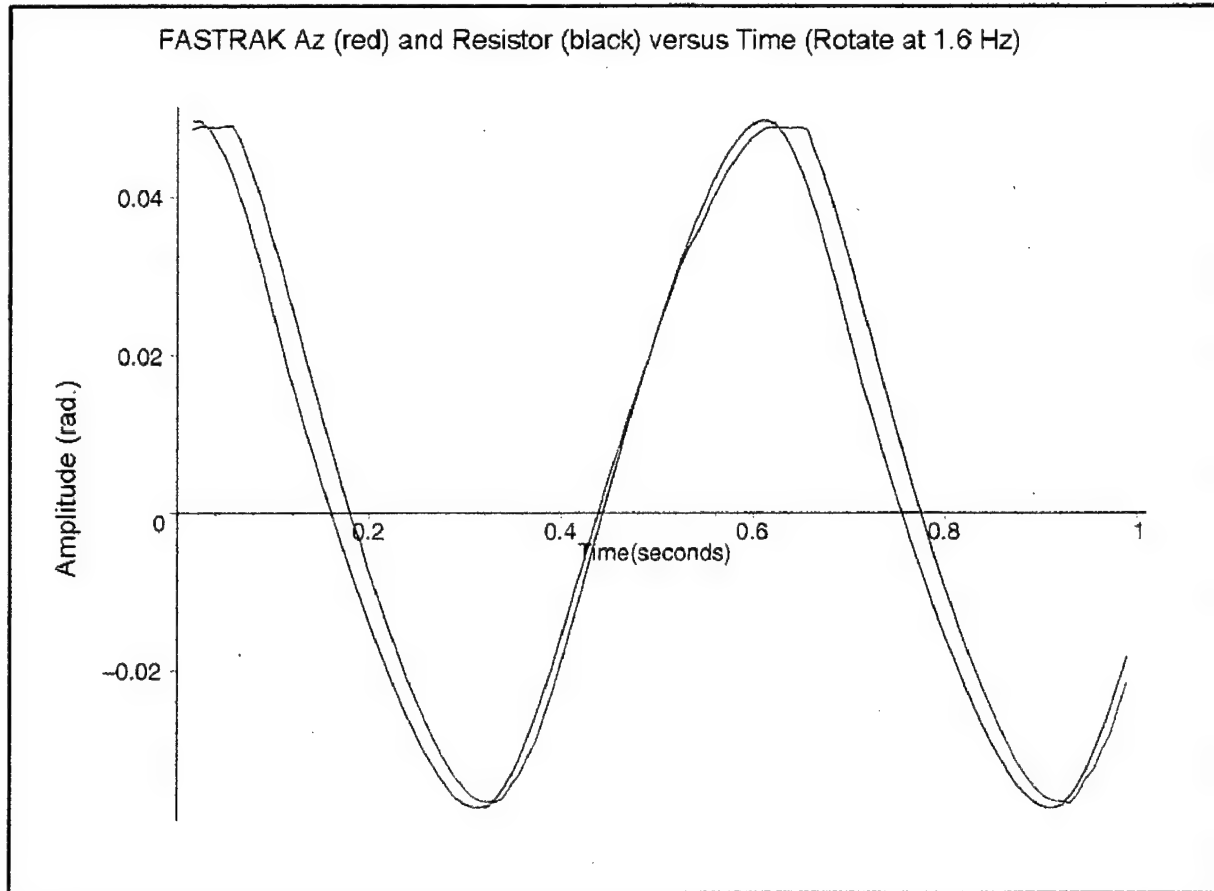FASTRAK® TRANSLATION VERSUS TIME

APPENDIX A

Description: The FASTRAK® X axis versus the analog sensor with sinusoidal translation at two different frequencies. The inner loop (red) is at 1.6 Hz. The outer loop (blue) is at 6.8 Hz. These loops are very close to the expected result if the latency is about 10 msec.
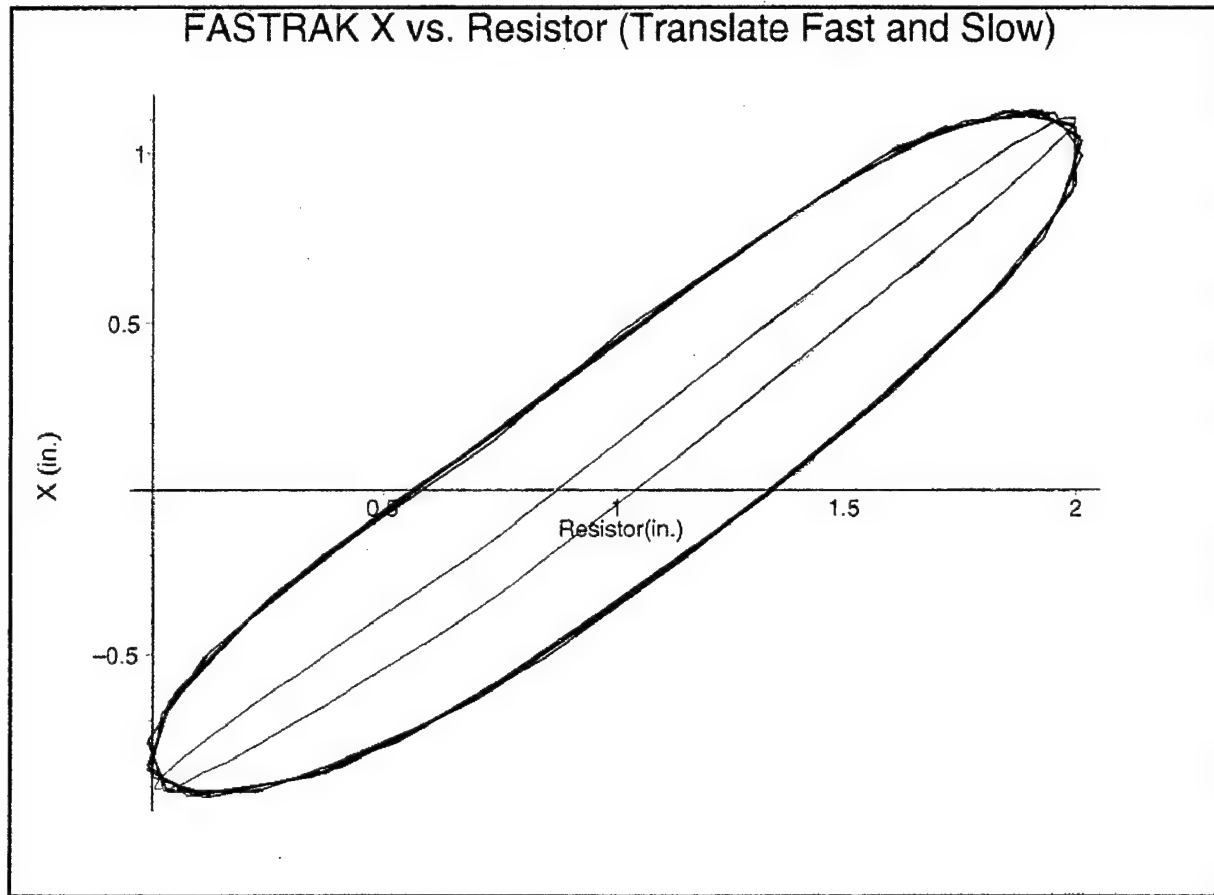
Figure A2.2
FASTRAK® TRANSLATION VERSUS ANALOG SENSOR
(CHANGING FREQUENCY)

Description: The azimuth output for the same test as figure A2.2. There is no input in rotation but the tracker interprets a rotation in azimuth as the receiver moves along the X axis. The flat loop (red) is at 1.6 Hz. And the large loop (blue) is at 6.8 Hz.
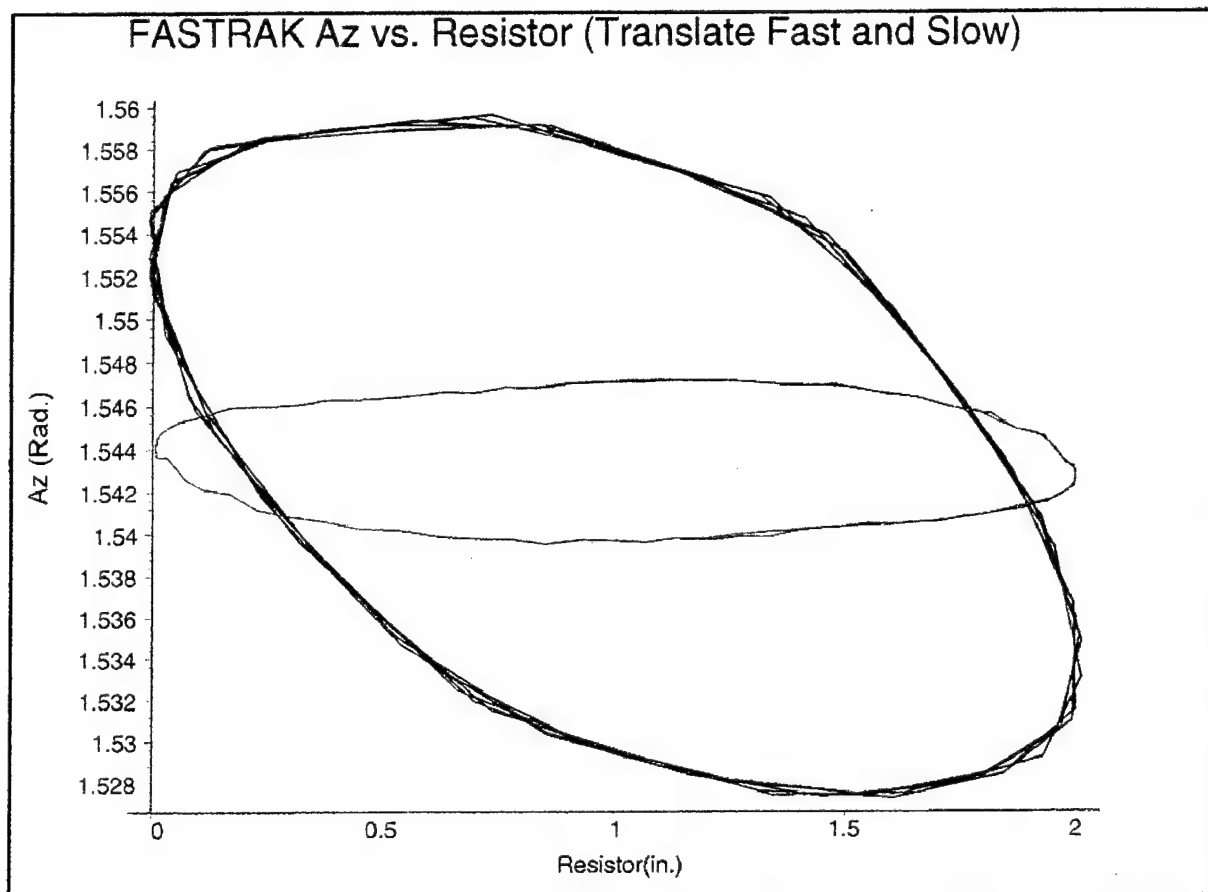
Figure A2.3
FASTRAK® NONSTIMULATED PARAMETER
(CHANGING FREQUENCY)

Description: The FASTRAK® X axis versus the analog sensor with sinusoidal translation at two different transmitter locations. The transmitter was 5 in. from the receiver in the top loop (red) and 21 in. from the receiver in the bottom loop (blue). The two loops are very similar as would be expected. The frequency is 1.6 Hz for both loops.
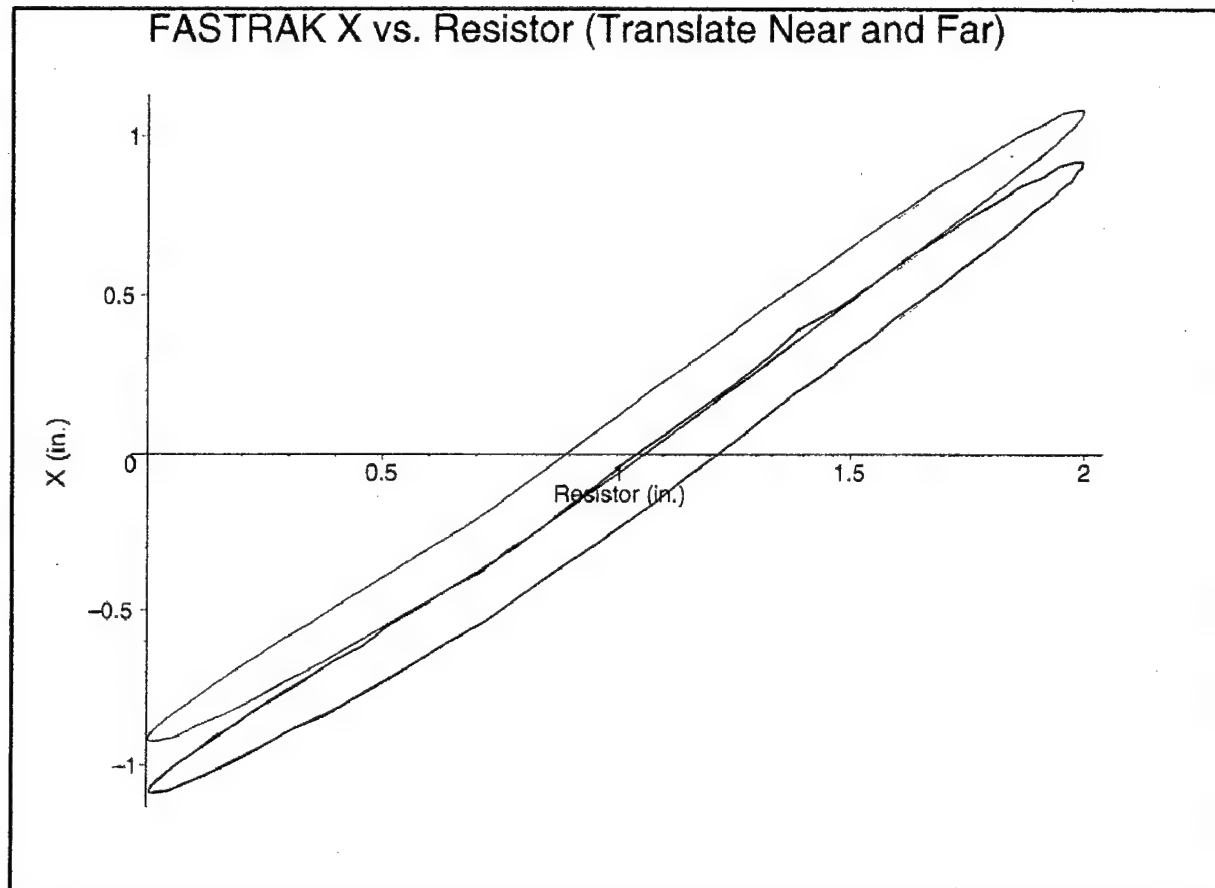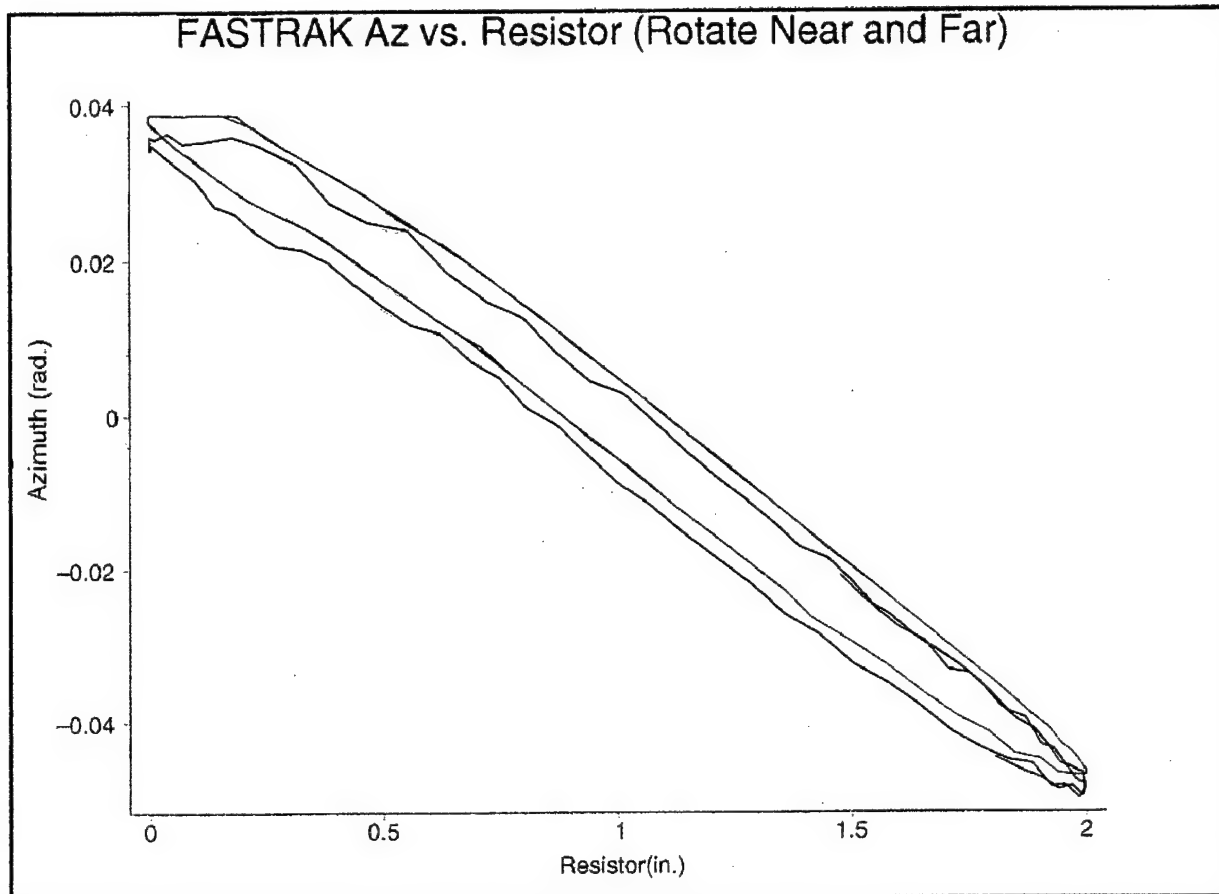

Figure A2.4
FASTRAK® TRANSLATION VERSUS ANALOG SENSOR
(CHANGING LOCATION)

23   APPENDIX A

Description: The azimuth output for the same test as A2.4. There is no input in azimuth. The outer loop (red) is the output in azimuth when the transmitter is 5 in. from the receiver and the flat loop (blue) is the output when the transmitter is 21 in. away. The frequency is 1.6 Hz for both loops.
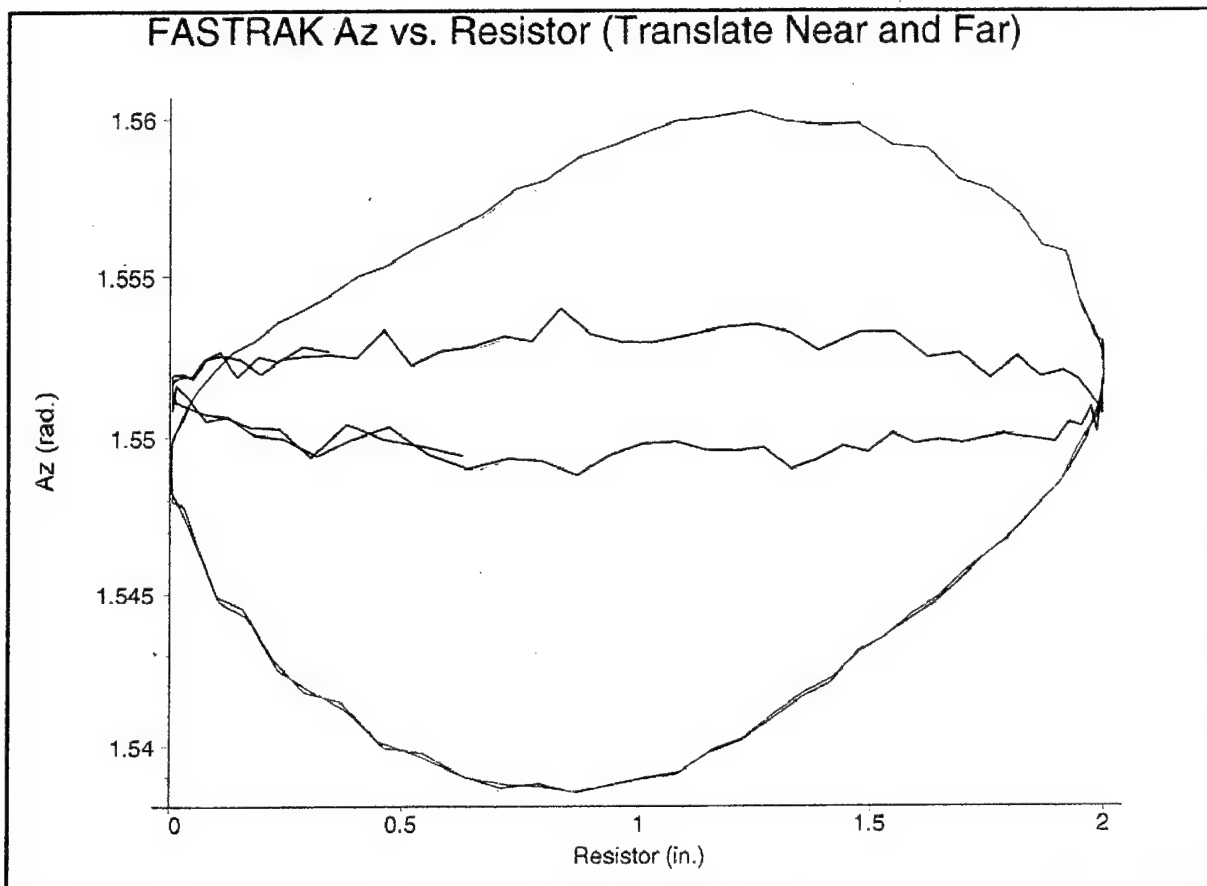
Figure A2.5
FASTRAK® NONSTIMULATED PARAMETER
(CHANGING LOCATION)

Description: The azimuth (red) and the analog sensor (black) versus Time. The input movement is sinusoidal rotation in azimuth at 1.6 Hz with 43.5 milliradians of amplitude. Parts of the curve match the input almost exactly while other parts show noticeable lag.

Figure A3.1
FASTRAK® ROTATION VERSUS TIME

Description: The FASTRAK® azimuth versus the analog sensor with sinusoidal rotation at two different frequencies. The inner loop (red) is at 1.7 Hz. The outer loop (blue) is at 6.7 Hz.
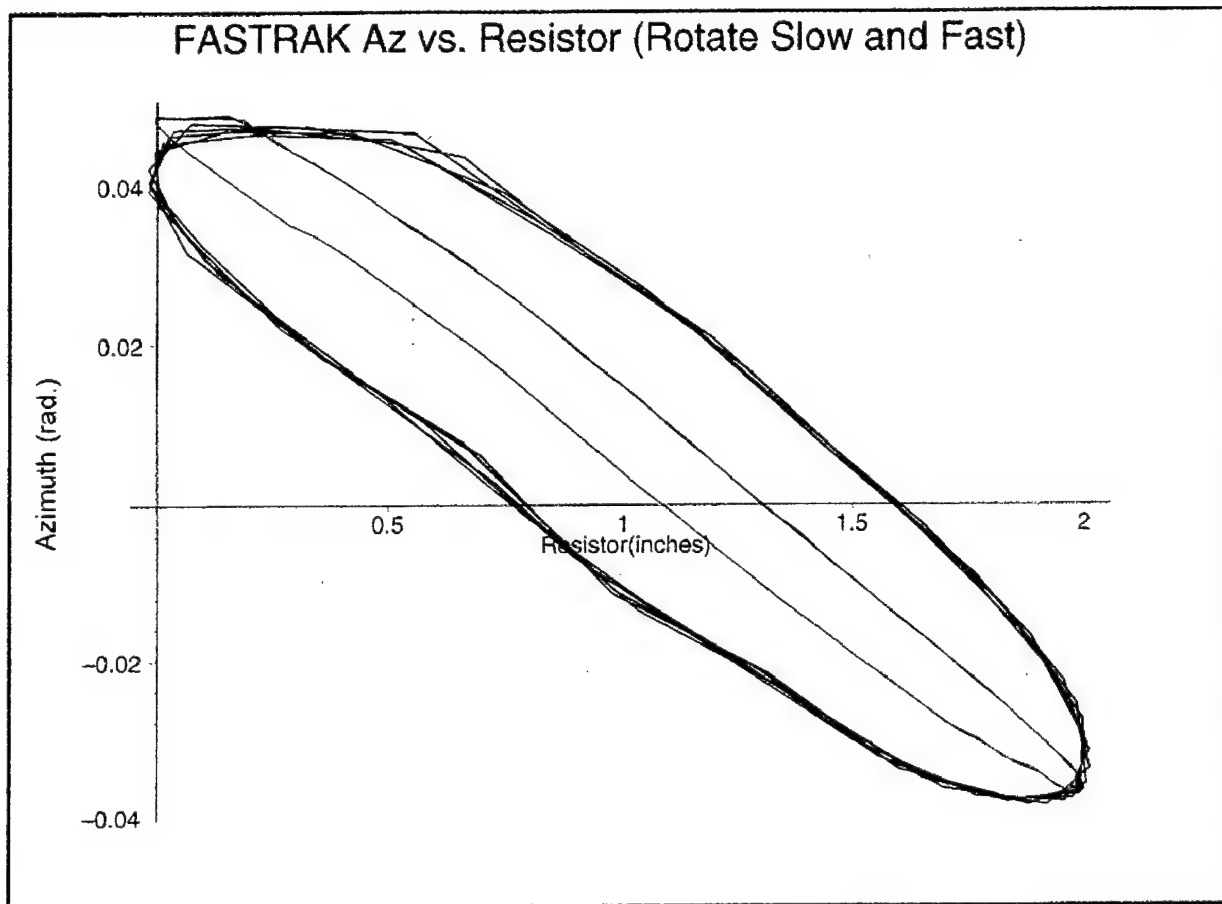
Figure A3.2
FASTRAK® ROTATION VERSUS ANALOG SENSOR
(CHANGING FREQUENCY)

Description: The azimuth versus the analog sensor with sinusoidal rotation at two different transmitter locations. The transmitter was 8 in. from the receiver in the smooth loop (red) and 27 in. from the receiver in the noisy loop (blue). The two loops are very similar as would be expected. The frequency is 1.6 Hz for both loops.

Figure A3.3
FASTRAK® ROTATION VERSUS ANALOG SENSOR
(CHANGING LOCATION)

Description: The azimuth versus the X axis as both parameters are stimulated in a sinusoidal motion. The inner loop (red) is at 1.4 Hz and the outer loop (blue) is at 6.0 Hz.
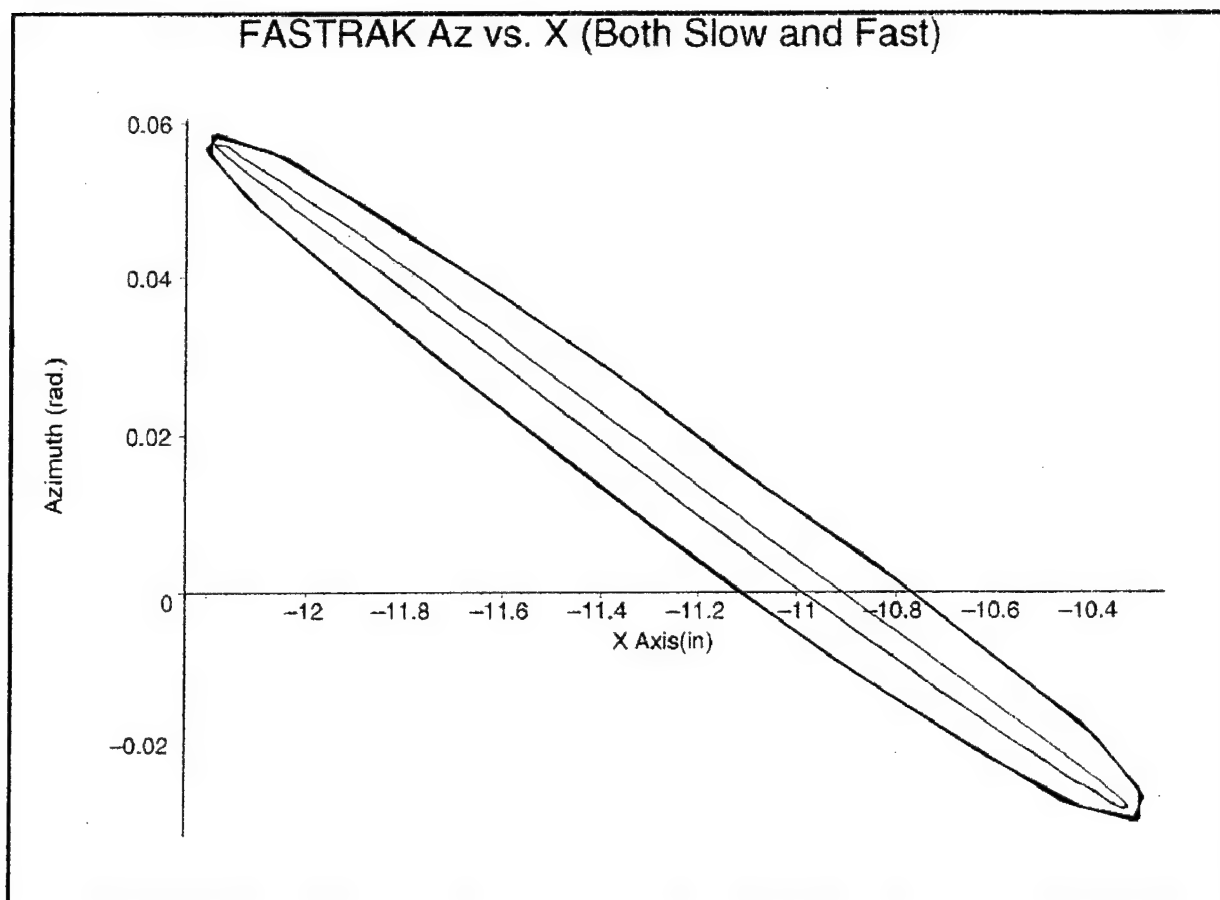
Figure A4.1
FASTRAK® ROTATION VERSUS TRANSLATION
(CHANGING FREQUENCY)

Description: The azimuth versus the X axis as both parameters are stimulated in a sinusoidal motion. A loop is apparent in the plot when the transmitter is near the receiver (red) but not when the transmitter is farther away (blue).

FASTRAK Az vs. X (Both Near and Far)
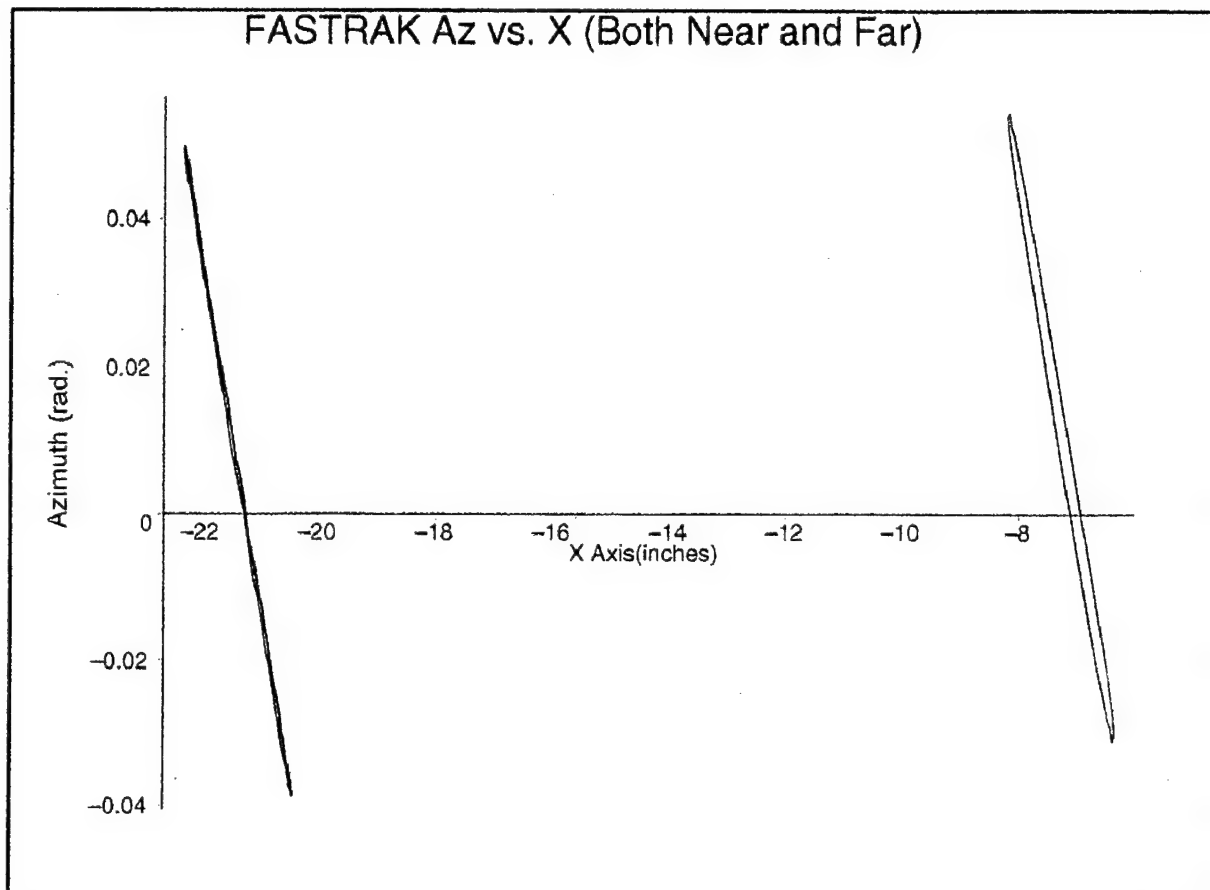
Figure A4.2
FASTRAK® ROTATION VERSUS TRANSLATION
(CHANGING LOCATION)

THIS PAGE INTENTIONALLY LEFT BLANK

APPENDIX B
FLOCK OF BIRDS® TESTS

Configuration:
Single transmitter
Single receiver
316 samples per second (103 updates per second)

NOTE: The difference between sample rate and update rate results in a stair step effect in the dynamic plots that should not be interpreted as noise. For tests in this appendix only, the FOB default output was on the "Y" axis. For all cases, alignment of the test items was comparable.

Default filters on.
RS-232 connection at 38,400 baud.

B1 Static Test
Figure B1.1 FOB (filters on) Static Precision in Position
Figure B1.2 FOB (filters on) Static Precision in Orientation

B2 Dynamic Translation Test
Figure B2.1 FOB (filters on) Translation versus Time
Figure B2.2 FOB (filters on) Translation versus Analog Sensor (Changing Frequency)
Figure B2.3 FOB (filters on) Nonstimulated Parameter (Changing Frequency)
Figure B2.4 FOB (filters on) Translation versus Analog Sensor (Changing Location)
Figure B2.5 FOB (filters on) Nonstimulated Parameter (Changing Location)

B3 Dynamic Rotation Test
Figure B3.1 FOB (filters on) Rotation versus Time
Figure B3.2 FOB (filters on) Rotation versus Analog Sensor (Changing Frequency)
Figure B3.3 FOB (filters on) Rotation versus Analog Sensor (Changing Location)

B4 Dynamic Translation and Rotation Test
Figure B4.1 FOB (filters on) Rotation versus Translation (Changing Frequency)
Figure B4.2 FOB (filters on) Rotation versus Translation (Changing Location)

Description: The RMS of the noise in position parameters as a function of distance between the transmitter and the receiver as measured along the X axis by the tracker. The filters substantially reduce the noise in all three position parameters X (red), Y (green), and Z (blue).
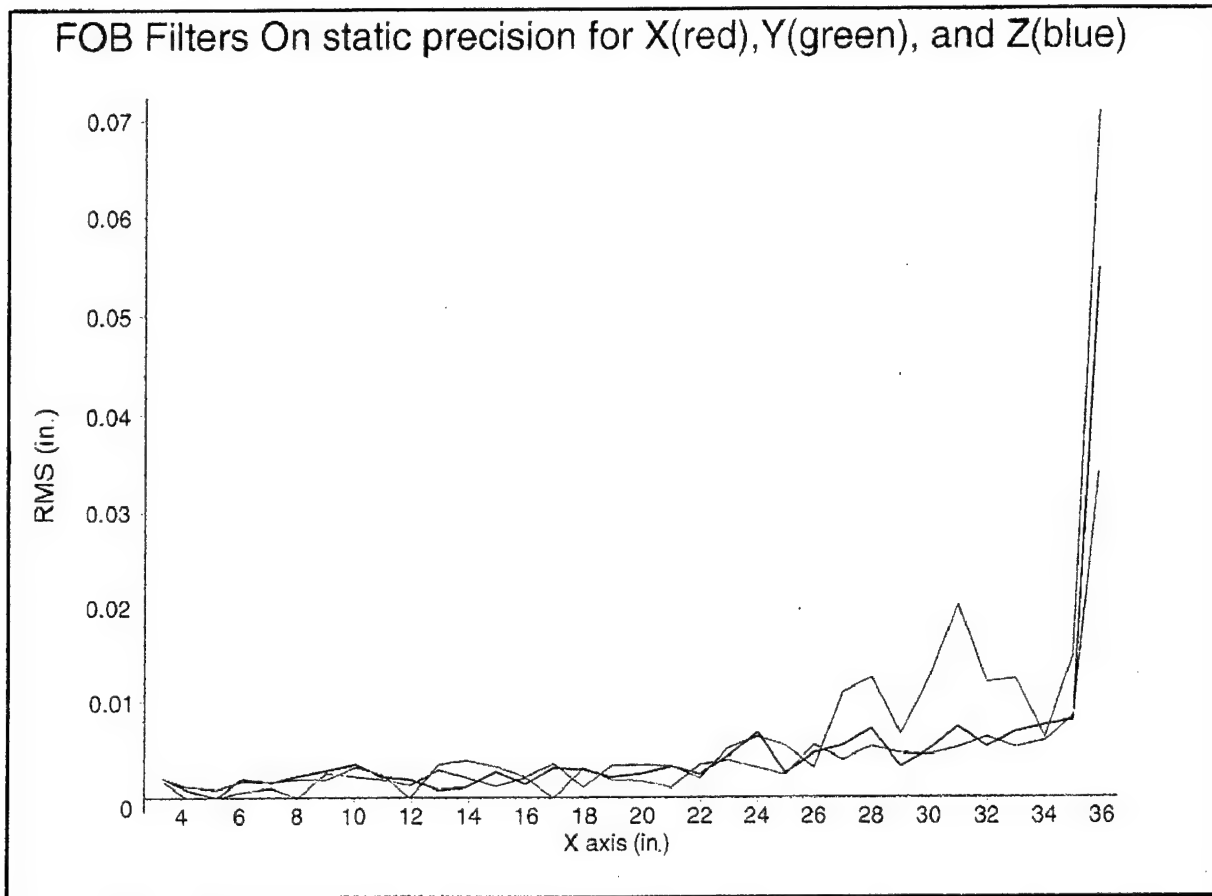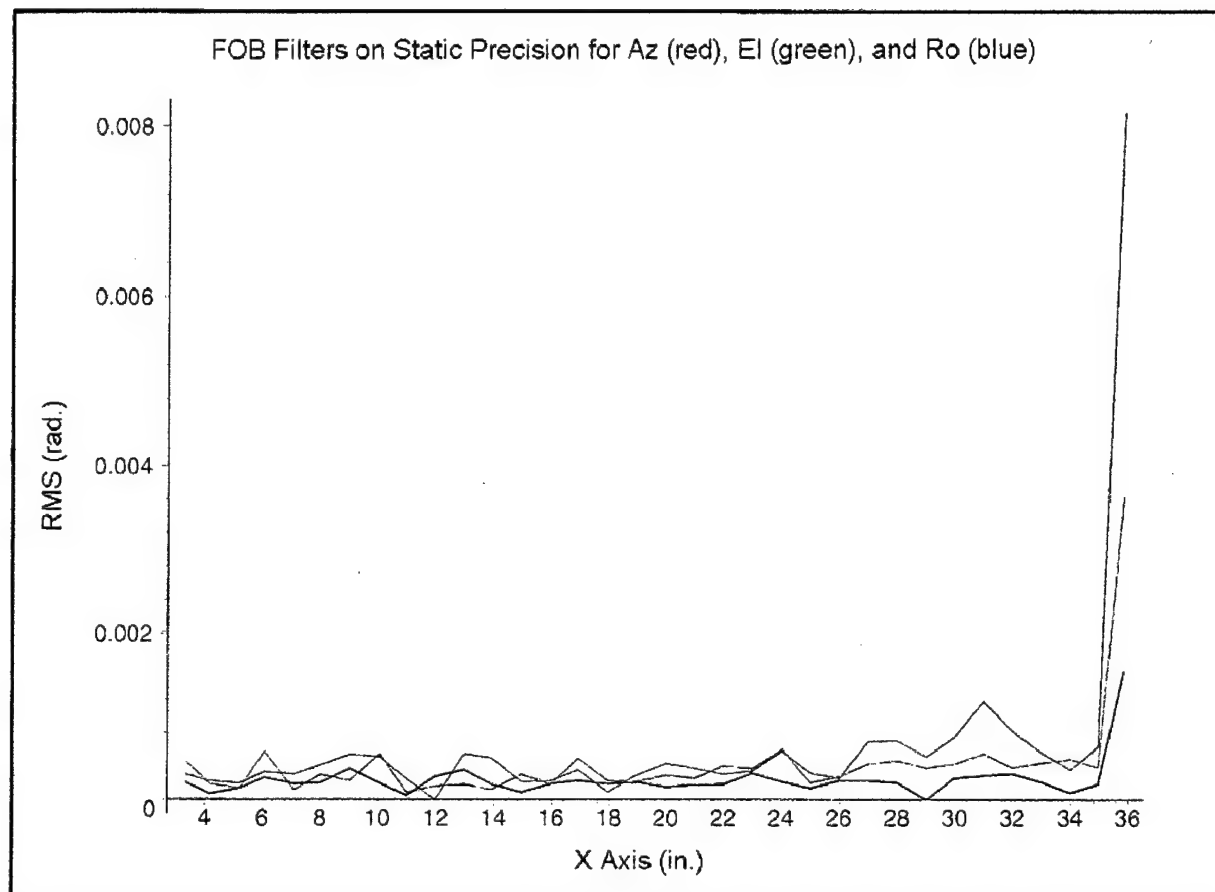

FOB Filters On static precision for X(red),Y(green), and Z(blue)

Figure B1.1
FOB (FILTERS ON) STATIC PRECISION IN POSITION

Description: The RMS of the noise in orientation parameters as a function of distance between the transmitter and the receiver as measured along the X axis by the tracker. The filters substantially reduce the noise in all three orientation parameters azimuth (red), elevation (green), and roll (blue).
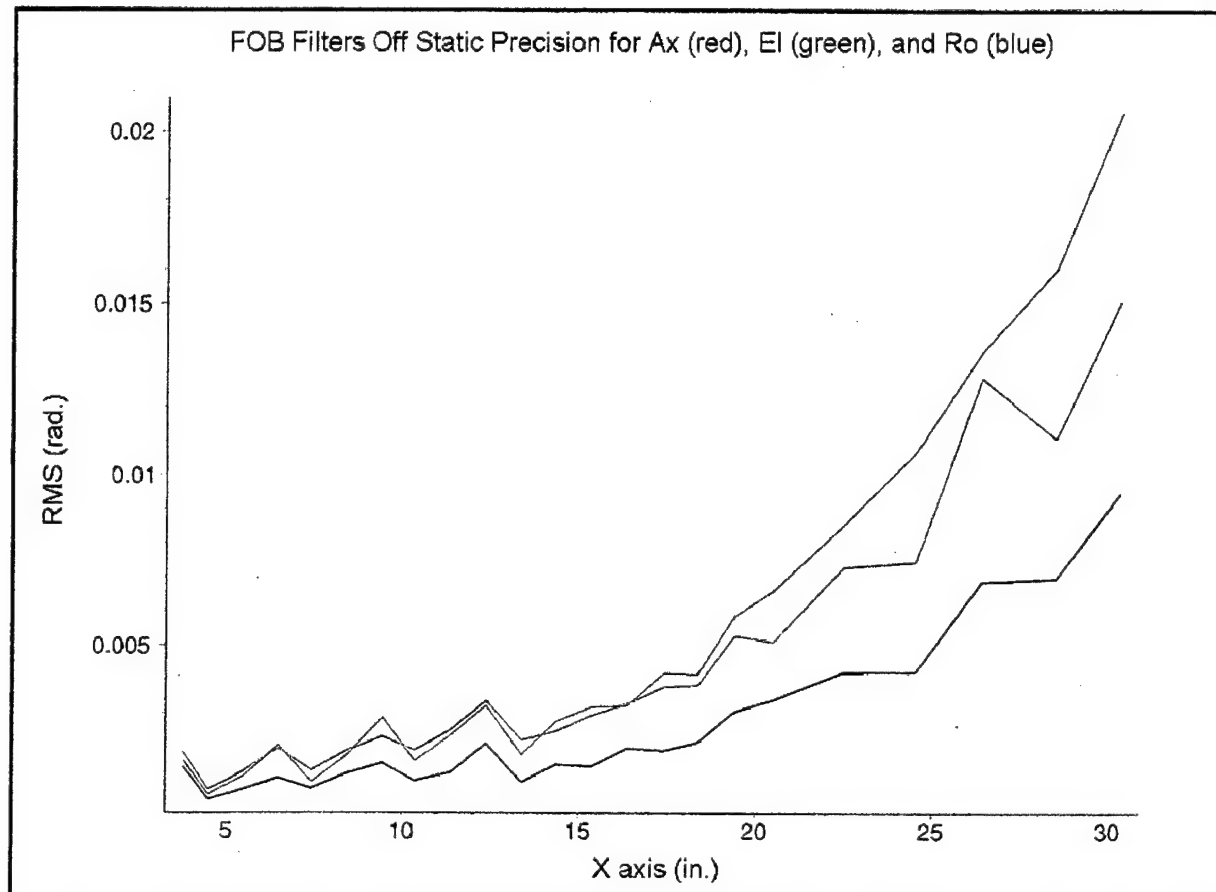

Figure B1.2
FOB (FILTERS ON) STATIC PRECISION IN ORIENTATION

Description: The FOB Y axis (red) and the analog sensor (black) versus time. The input movement is sinusoidal translation along the Y axis at 1.6 Hz with 1 in. of amplitude. A substantial lag is apparent throughout the curve with additional distortions at the points of reversal.
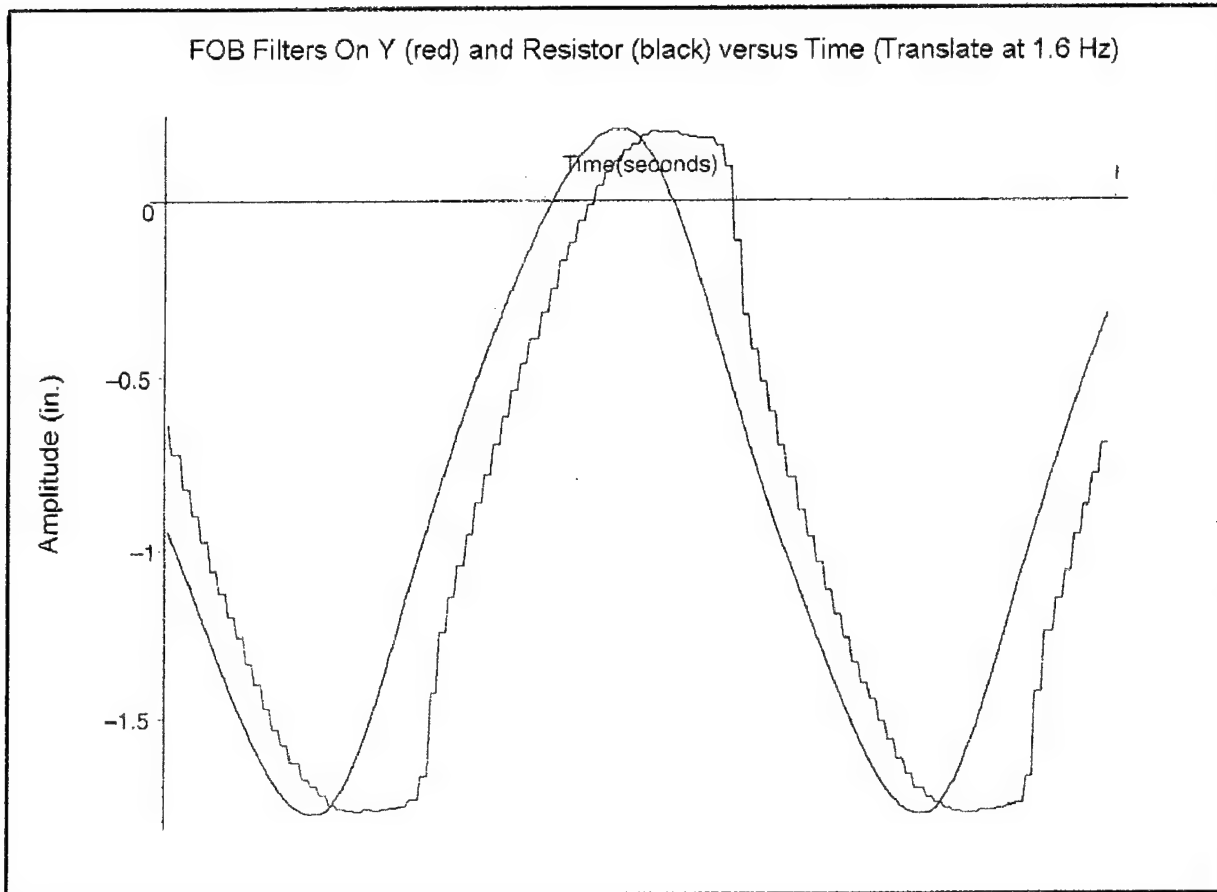
Figure B2.1
FOB (FILTERS ON) TRANSLATION VERSUS TIME

Description: The RMS of the noise in orientation parameters as a function of distance between the transmitter and the receiver as measured along the X axis by the tracker. Without the filters, the noise increases rapidly in all three orientation parameters azimuth (red), elevation (green), and Roll (blue) as distance increases.

Figure C1.2
FOB (FILTERS OFF) STATIC PRECISION IN ORIENTATION

Description: The X axis (red) and the analog sensor (black) versus time. The input movement is sinusoidal translation along the X axis at 1.6 Hz with 1 in. of amplitude. A lag is apparent throughout most of the curve but it is substantially less than the lag with filters on (see figure B2.1).

FOB Filters Off X (red) and Resistor (black) versus Time Translate at 1.6 Hz)
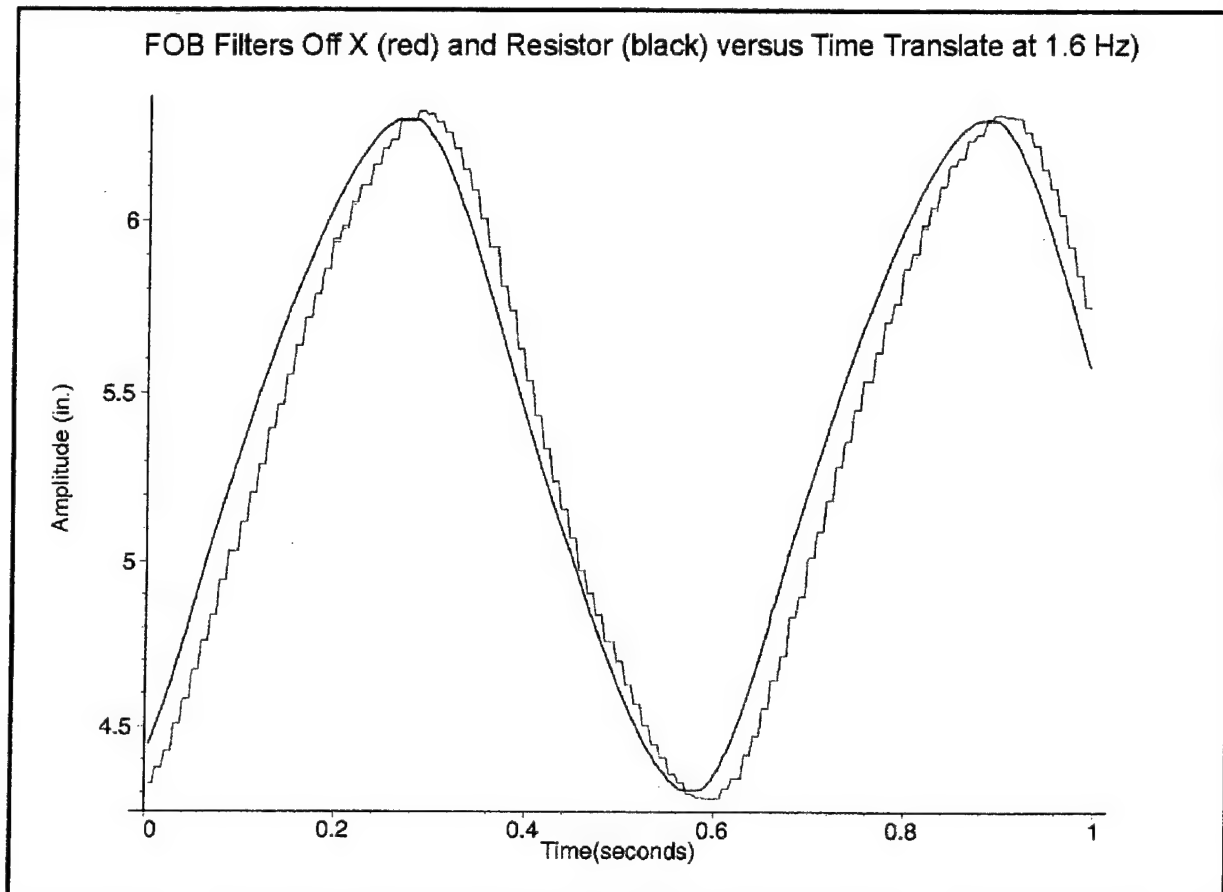
Figure C2.1
FOB (FILTERS OFF) TRANSLATION VERSUS TIME

Description: The X axis versus the analog sensor with sinusoidal translation at two different frequencies. The inner loop (red) is at 1.6 Hz. The outer loop (blue) is at 7.2 Hz.
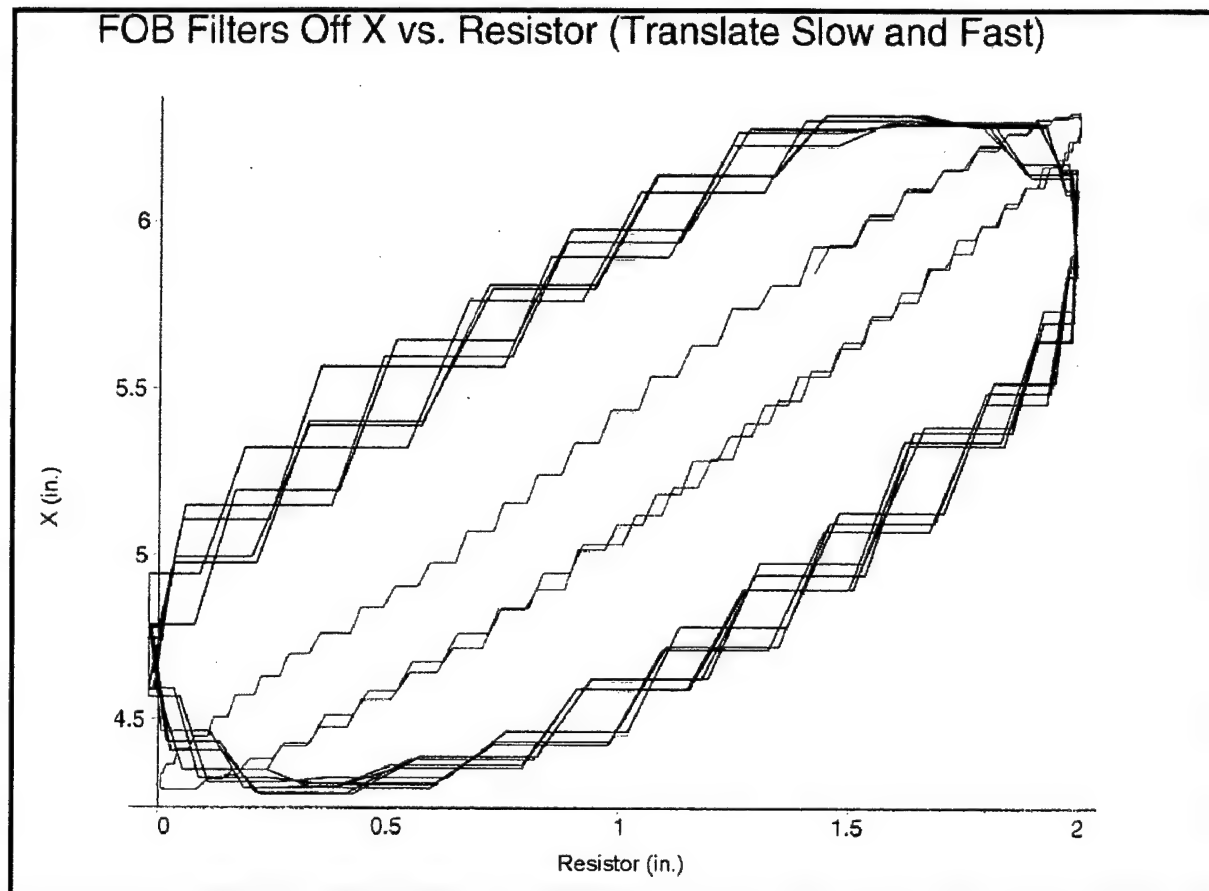
Figure C2.2
FOB (FILTERS OFF) TRANSLATION VERSUS ANALOG SENSOR
(CHANGING FREQUENCY)

Description: The azimuth versus the analog sensor as receiver is translated along the X axis. There is no input rotation in azimuth. The flat loop (red) is at 1.6 Hz and the slanted loop (blue) is at 7.2 Hz.
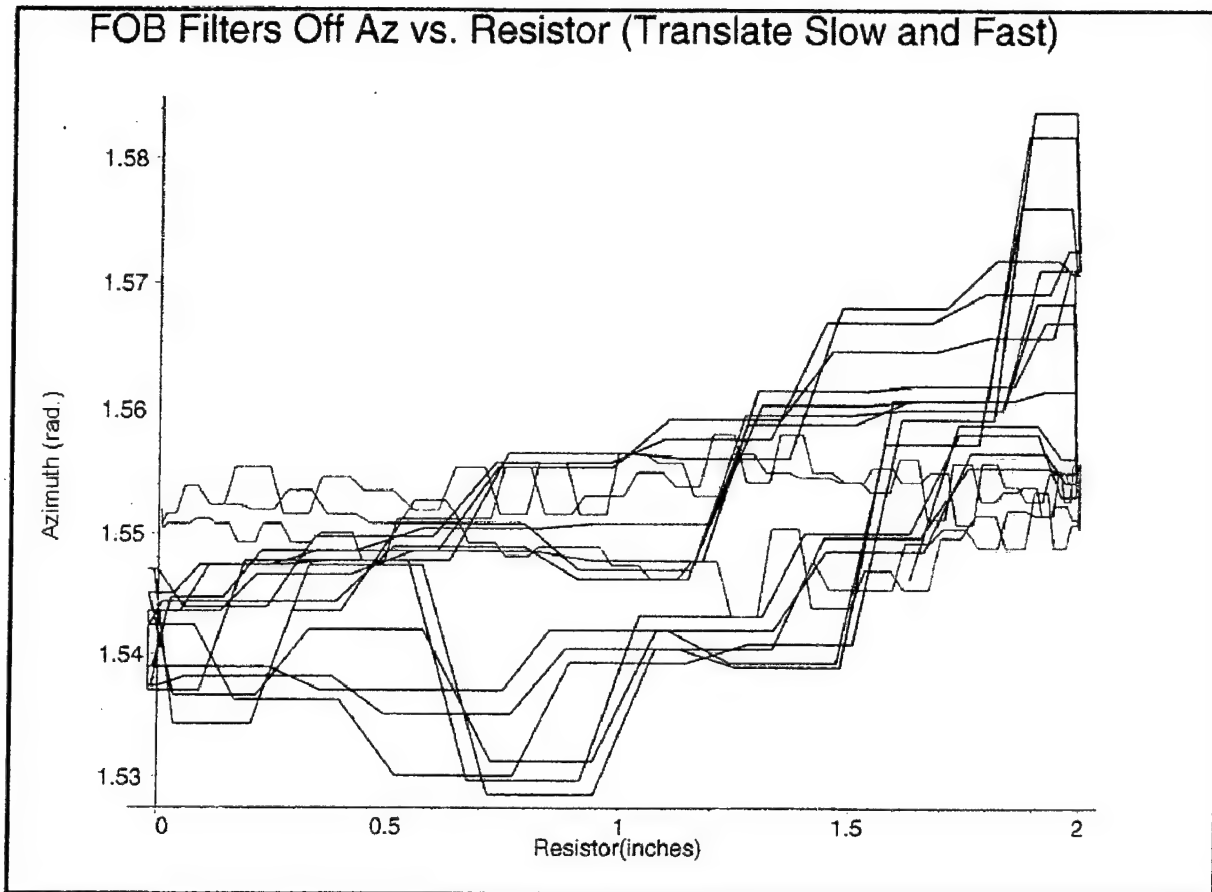
Figure C2.3
FOB (FILTERS OFF) NONSTIMULATED PARAMETER
(CHANGING FREQUENCY)

Description: The X axis versus the analog sensor with the transmitter at two different locations. The transmitter is 4 in. away from the receiver in the upper loop (red) and 21 in. away for the lower loop (blue). Both loops are at 1.6 Hz.
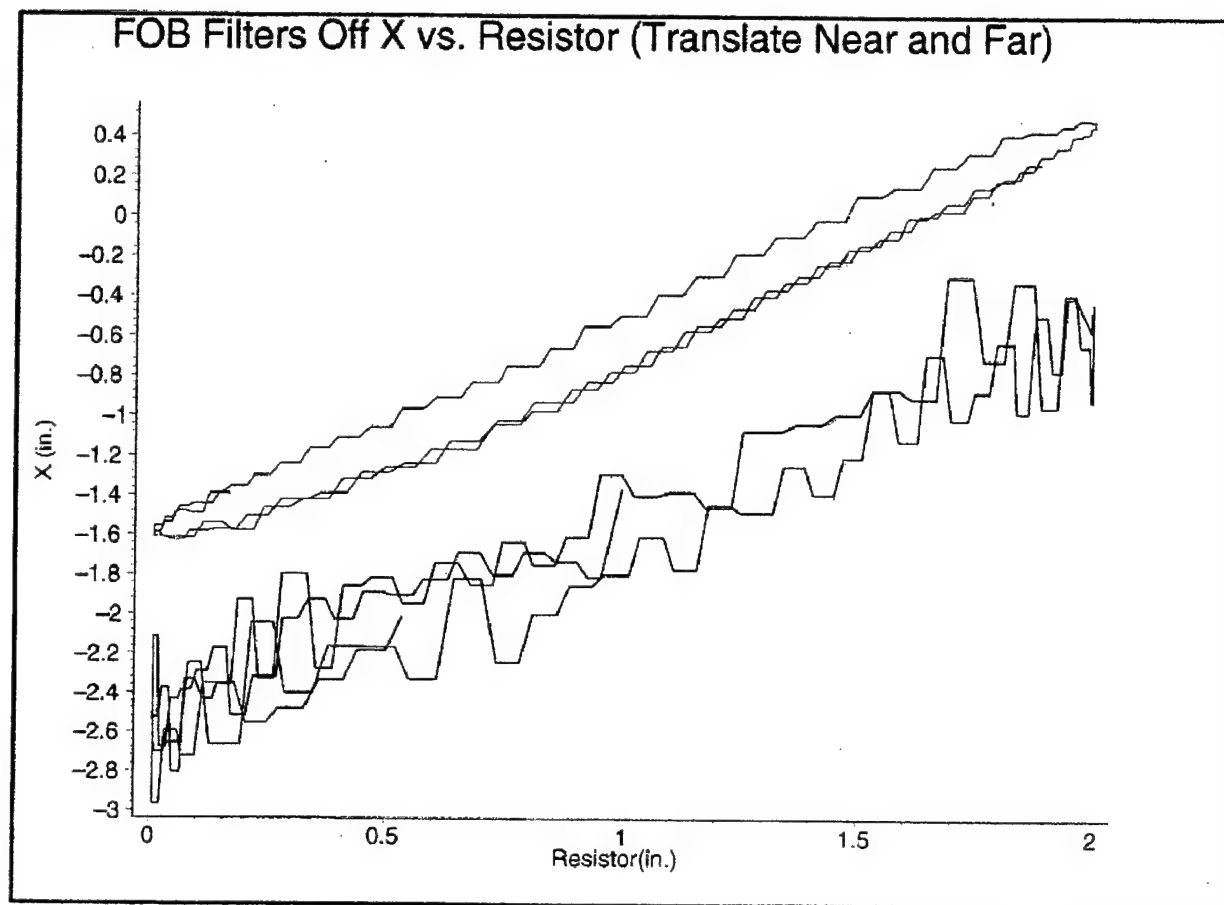
Figure C2.4
FOB (FILTERS OFF) TRANSLATION VERSUS ANALOG SENSOR
(CHANGING LOCATION)

Description: The azimuth output for the same test as C2.4. There is no input in azimuth. The lower loop (red) is the output in azimuth when the transmitter is 4 in. from the receiver and the upper loop (blue) is the output when the transmitter is 21 in. away. The frequency is 1.6 Hz for both loops.
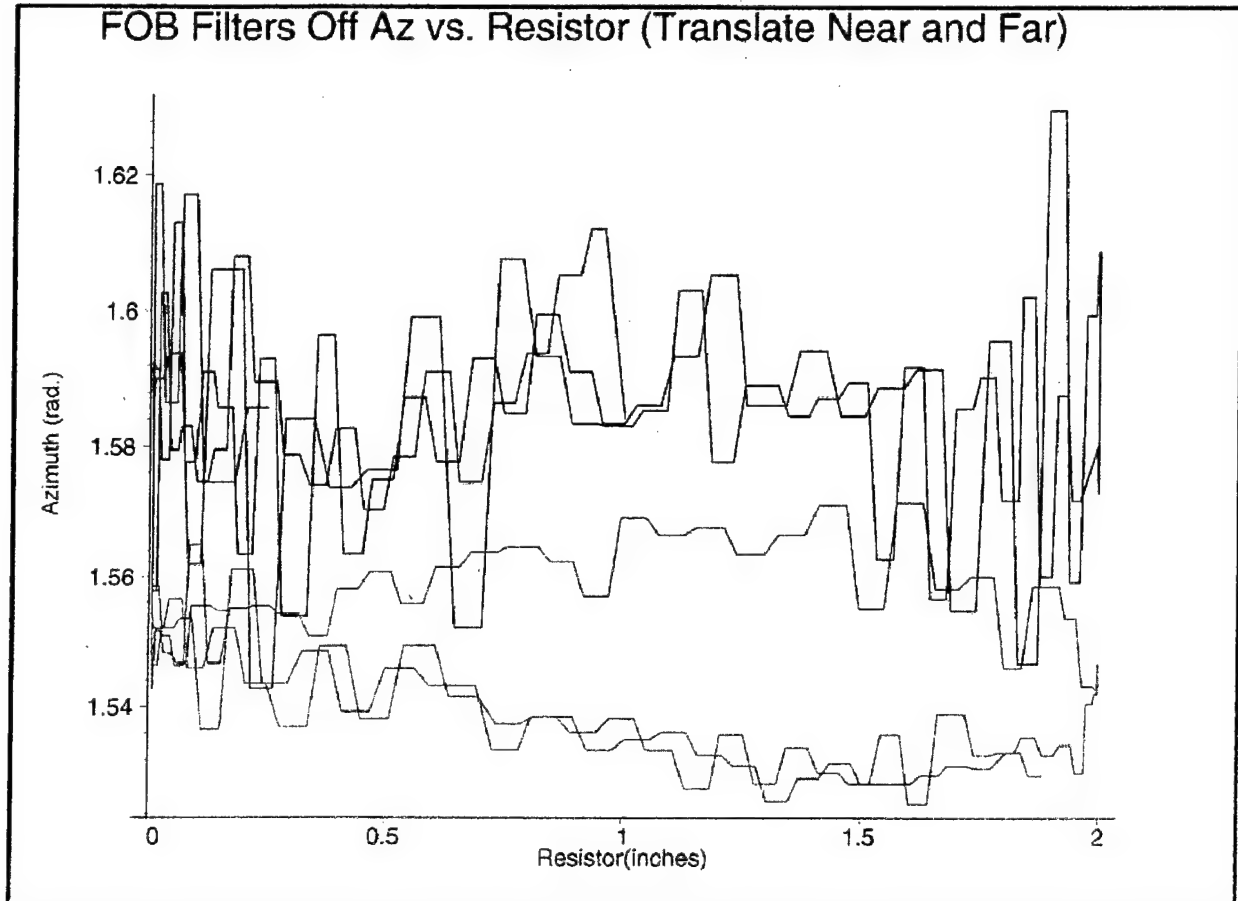
Figure C2.5
FOB (FILTERS OFF) NONSTIMULATED PARAMETER
(CHANGING LOCATION)

Description: The azimuth (red) and the analog sensor (black) versus Time. The input movement is sinusoidal rotation in azimuth at 1.6 Hz with 43.5 milliradians of amplitude. Noise dominates the curve making it difficult to assess latency.
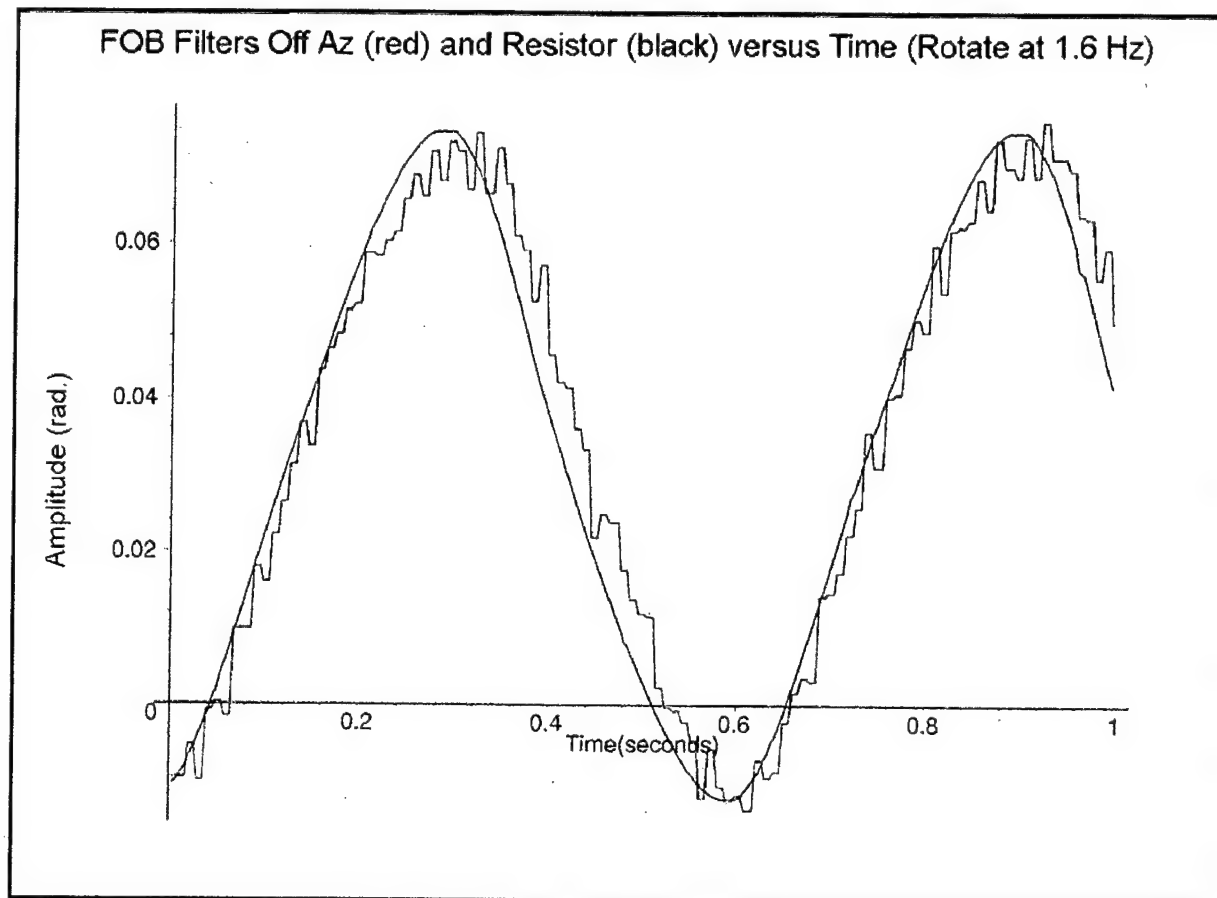
Figure C3.1
FOB (FILTERS OFF) ROTATION VERSUS TIME

APPENDIX C

Description: The azimuth versus the analog sensor with sinusoidal rotation at two different frequencies. The inner loop (red) is at 1.7 Hz. The outer loop (blue) is at 7.4 Hz.
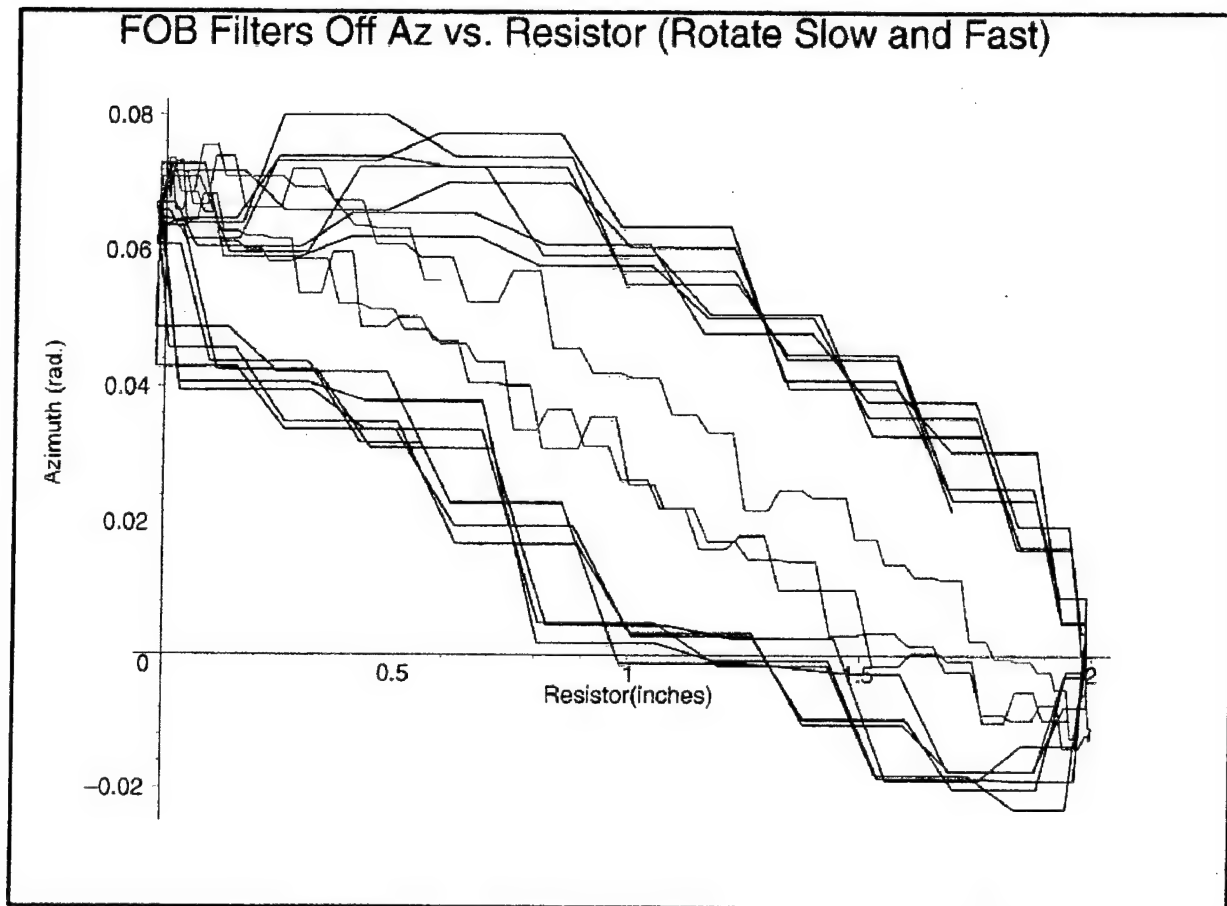

Figure C3.2
FOB (FILTERS OFF) ROTATION VERSUS ANALOG SENSOR
(CHANGING FREQUENCY)

Description: The azimuth versus the analog sensor with sinusoidal rotation at two different transmitter locations. The transmitter was 8 in. from the receiver in the smooth loop (red) and 27 in. from the receiver in the noisy loop (blue).
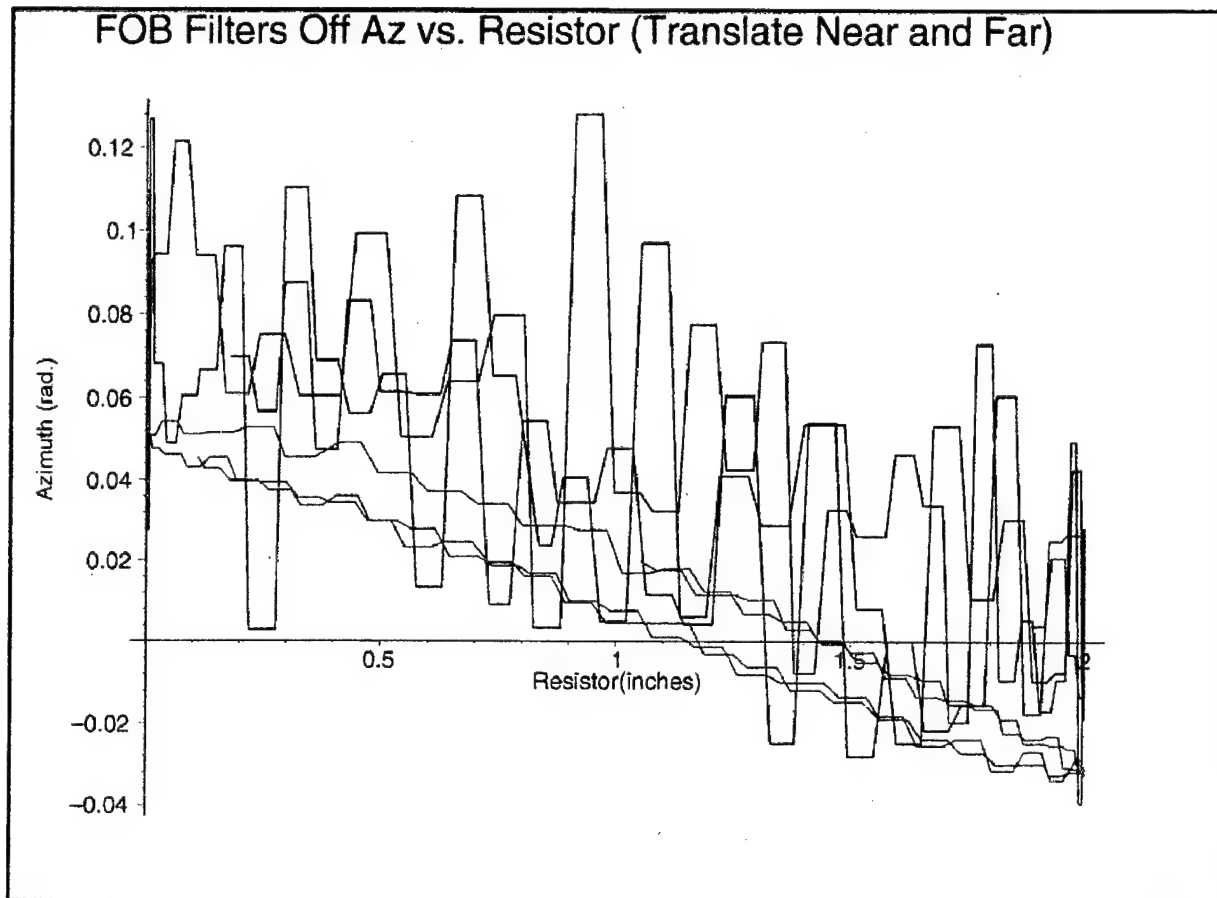

Figure C3.3
FOB (FILTERS OFF) ROTATION VERSUS ANALOG SENSOR
(CHANGING LOCATION)

APPENDIX C

Description: The azimuth versus the X axis as both parameters are stimulated in a sinusoidal motion. The thin loops indicate that there is almost no lag between the two parameters. The inner loop (red) is at 1.9 Hz and the outer loop (blue) is at 6.5 Hz.
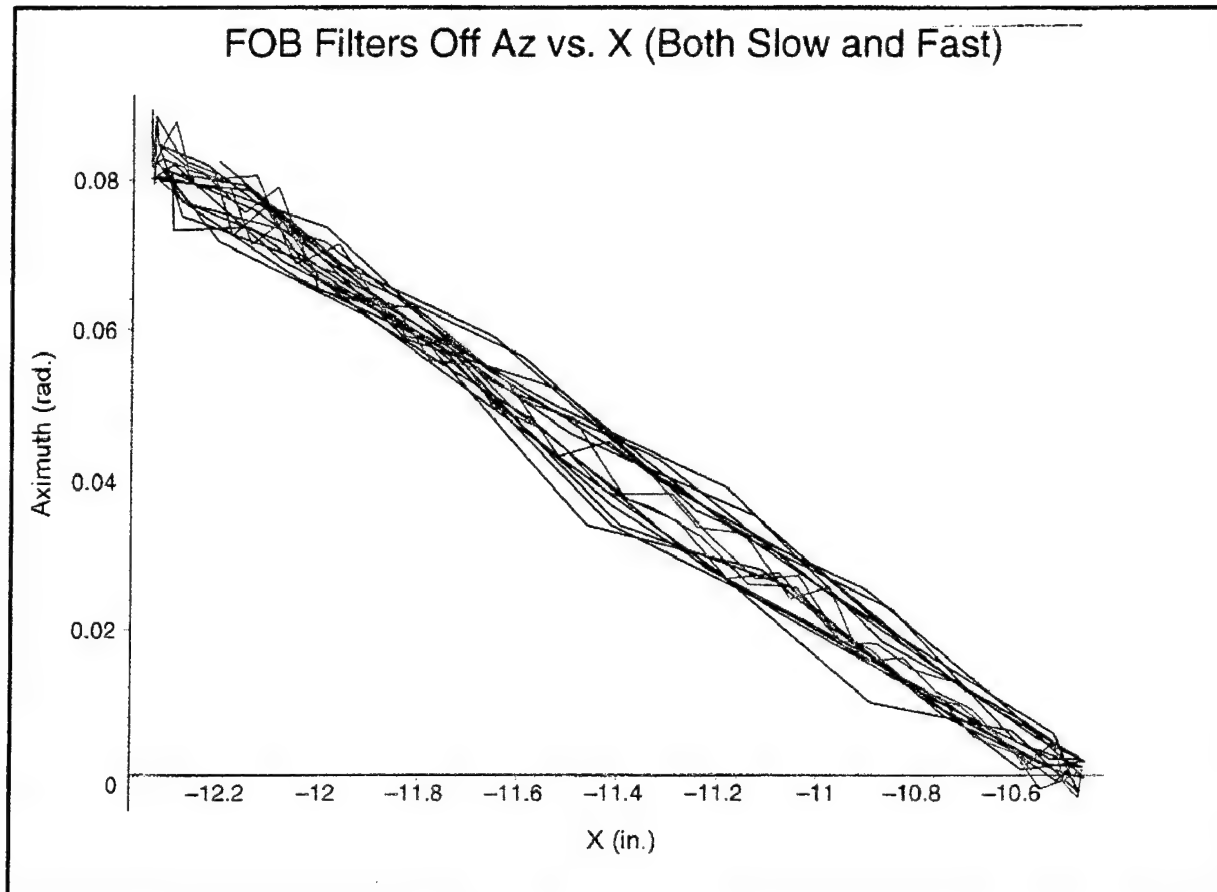

Figure C4.1
FOB (FILTERS OFF) ROTATION VERSUS TRANSLATION
(CHANGING FREQUENCY)

Description: The azimuth versus the X axis with the transmitter at two different locations. The noise in the far loop (blue) doubles range of azimuth readings from the near loop (red).
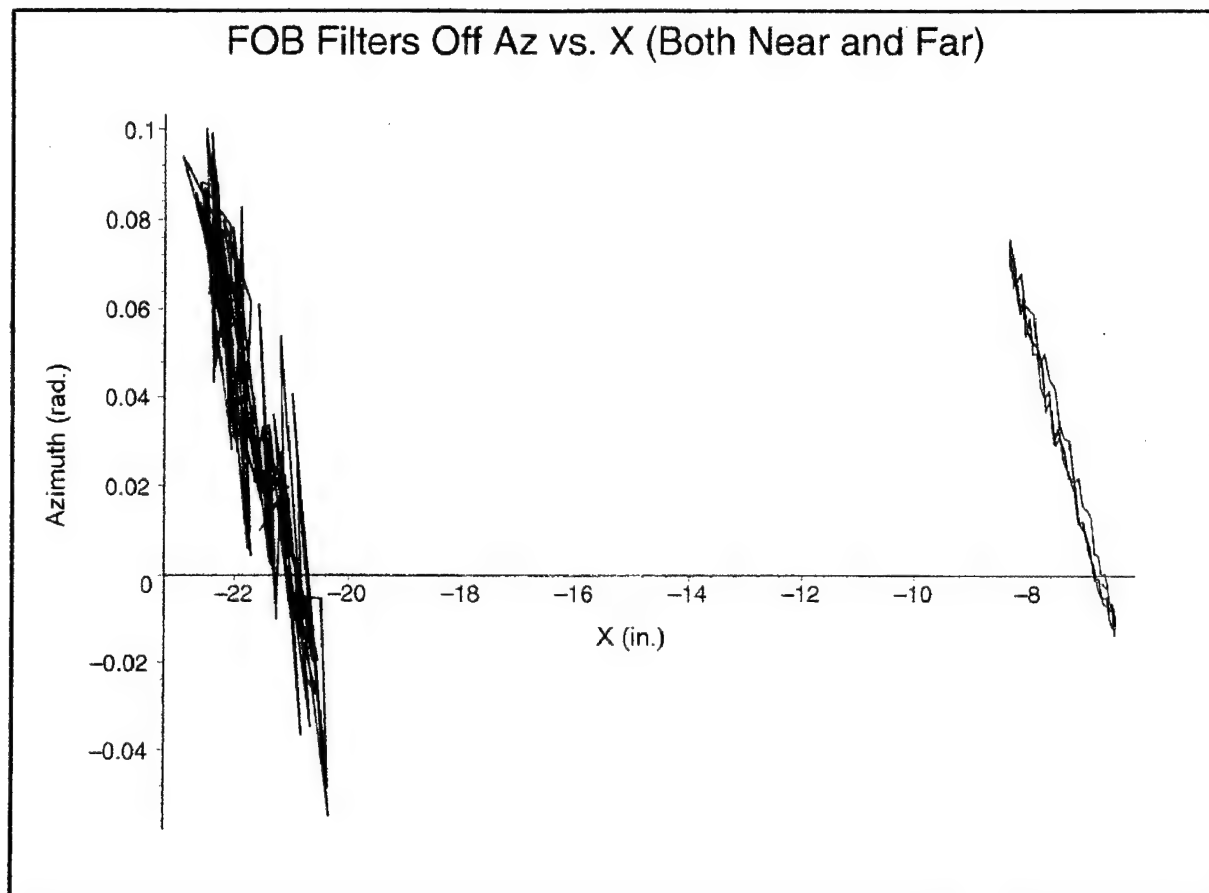

Figure C4.2
FOB (FILTERS OFF) ROTATION VERSUS TRANSLATION
(CHANGING LOCATION)

THIS PAGE INTENTIONALLY LEFT BLANK

Description: The Y axis versus the analog sensor with sinusoidal translation at two different frequencies. The inner loop (red) is at 1.6 Hz. The outer loop (blue) is at 6.1 Hz. Substantial phase lag is apparent, as well as perturbations in the shape of both loops.
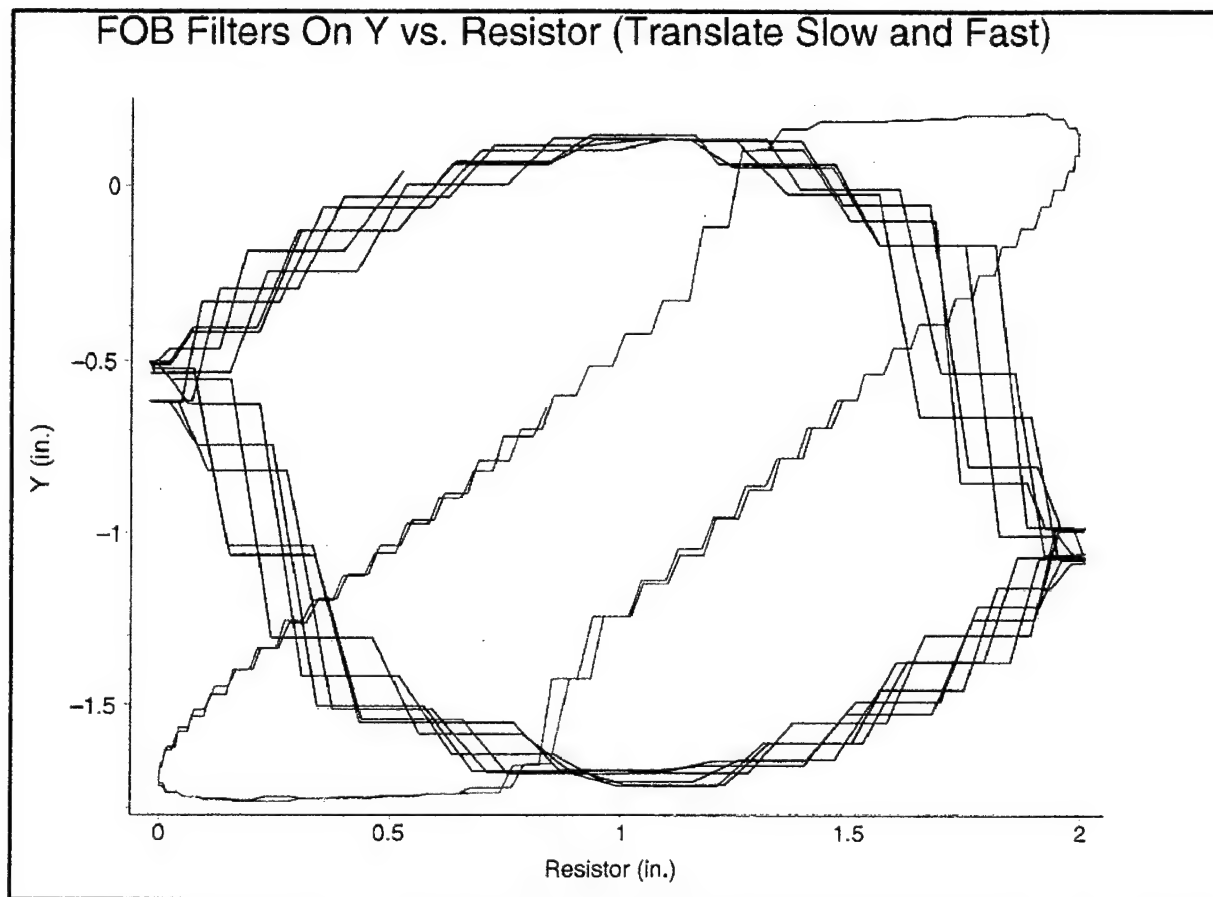

Figure B2.2
FOB (FILTERS ON) TRANSLATION VERSUS ANALOG SENSOR
(CHANGING FREQUENCY)

Description: The azimuth versus the analog sensor as receiver is translated along the Y axis. There is no input rotation in azimuth. The flat loop (red) is at 1.6 Hz and the slanted loop (blue) is at 6.1 Hz.
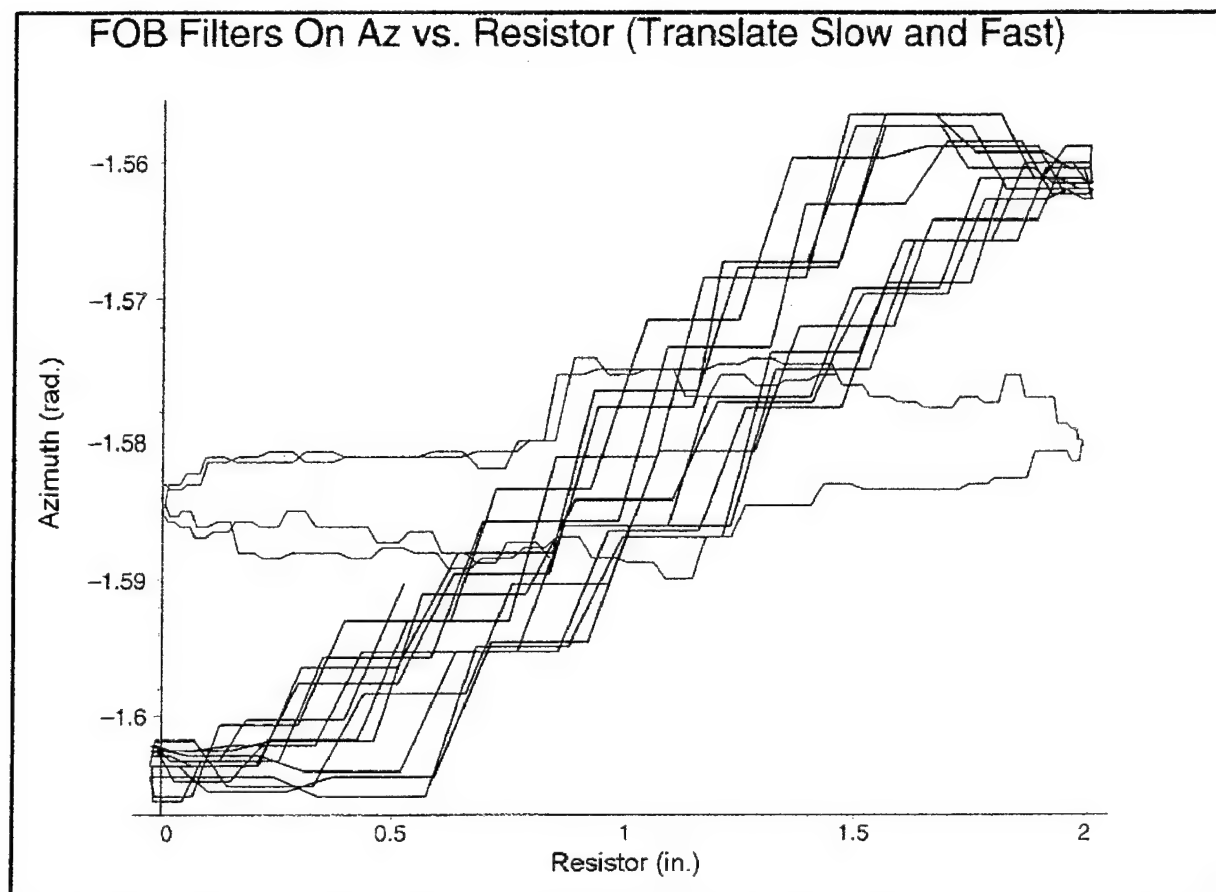

Figure B2.3
FOB (FILTERS ON) NONSTIMULATED PARAMETER
(CHANGING FREQUENCY)

Description: The Y axis versus the analog sensor with the transmitter at two different locations. The transmitter is 4 in. away from the receiver in the taller loop (red) and 21 in. away for the shorter loop (blue). Both loops are at 1.6 Hz.
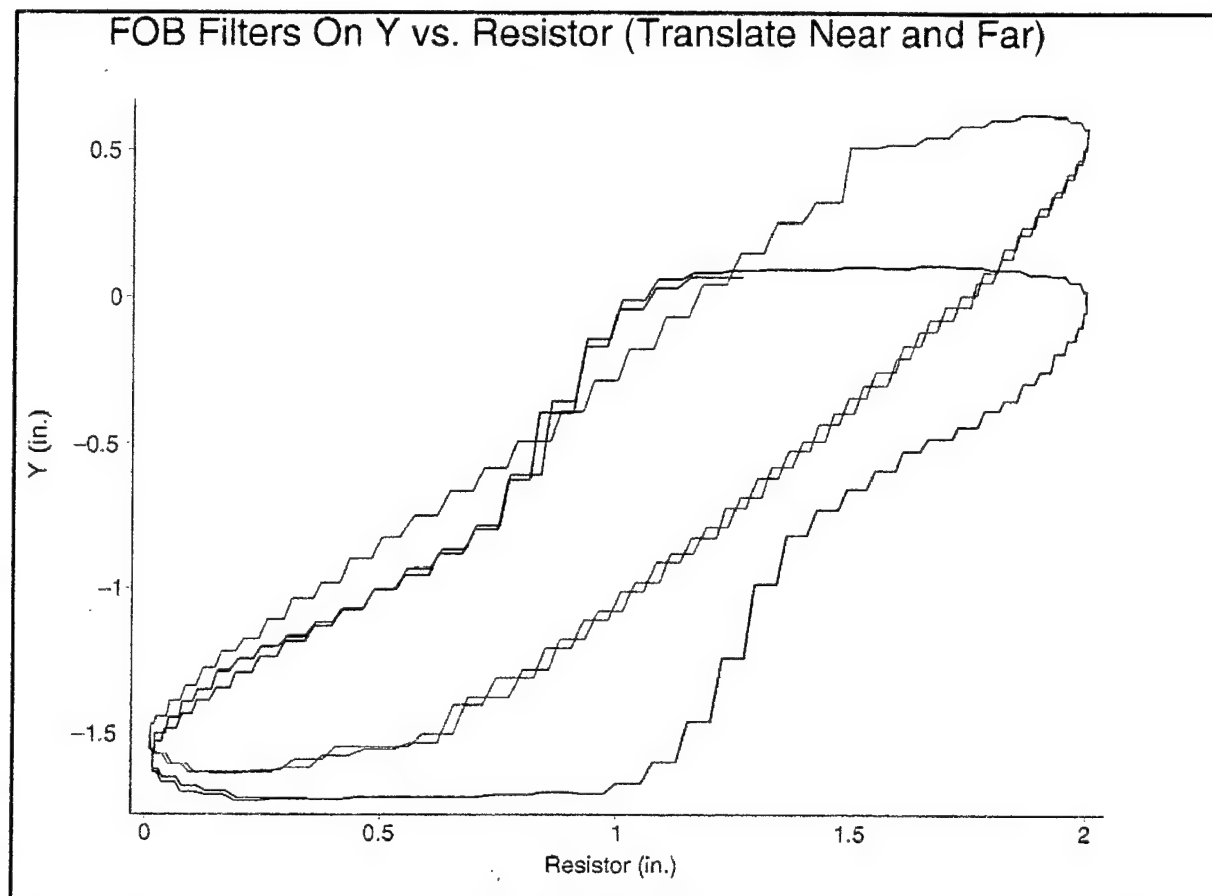

Figure B2.4
FOB (FILTERS ON) TRANSLATION VERSUS ANALOG SENSOR
(CHANGING LOCATION)

Description: The azimuth output for the same test as B2.4. There is no input in azimuth. The outer loop (red) is the output in azimuth when the transmitter is 4 in. from the receiver and the flat loop (blue) is the output when the transmitter is 21 in. away. The frequency is 1.6 Hz for both loops.
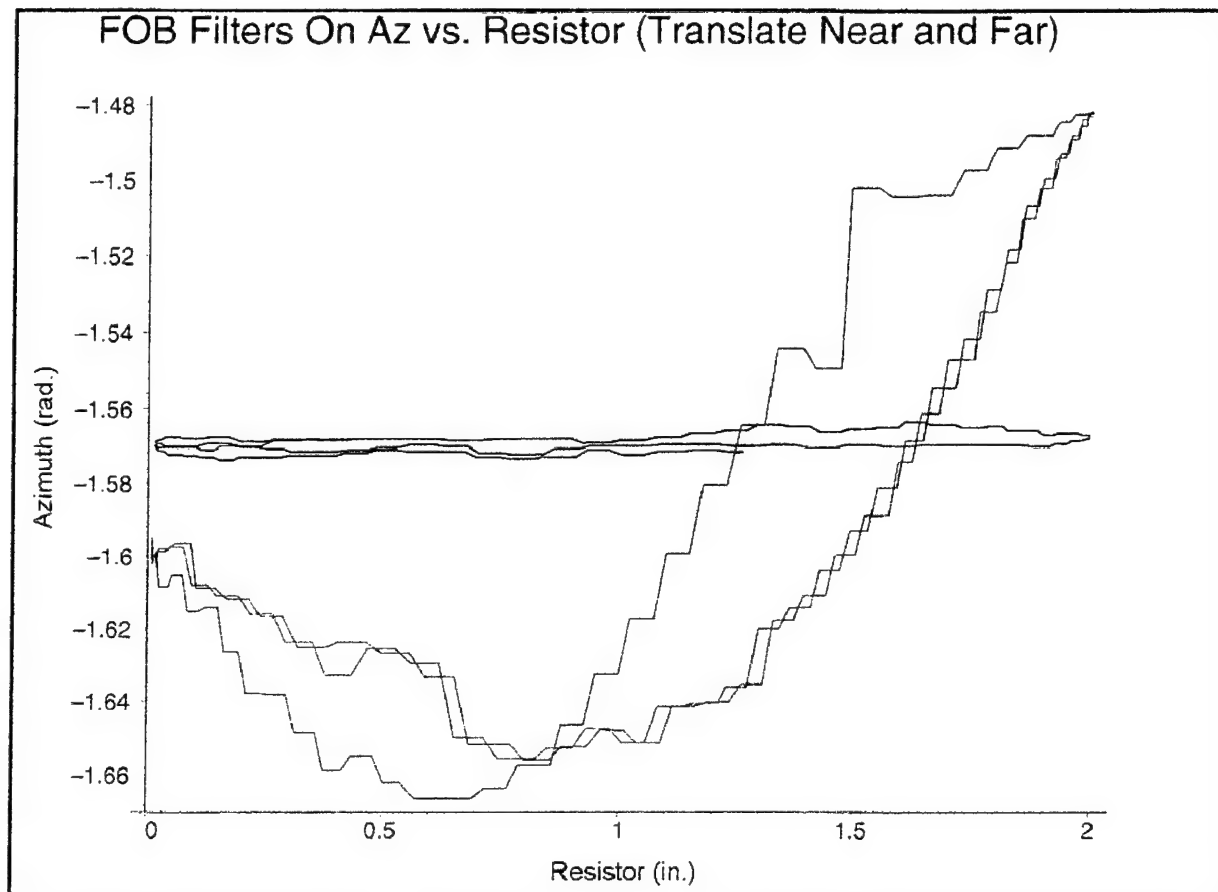

Figure B2.5
FOB (FILTERS ON) NONSTIMULATED PARAMETER
(CHANGING LOCATION)

APPENDIX B

Description: The azimuth (red) and the analog sensor (black) versus Time. The input movement is sinusoidal rotation in azimuth at 1.6 Hz with 43.5 milliradians of amplitude. A substantial lag is apparent throughout the curve with additional distortions at the points of reversal.
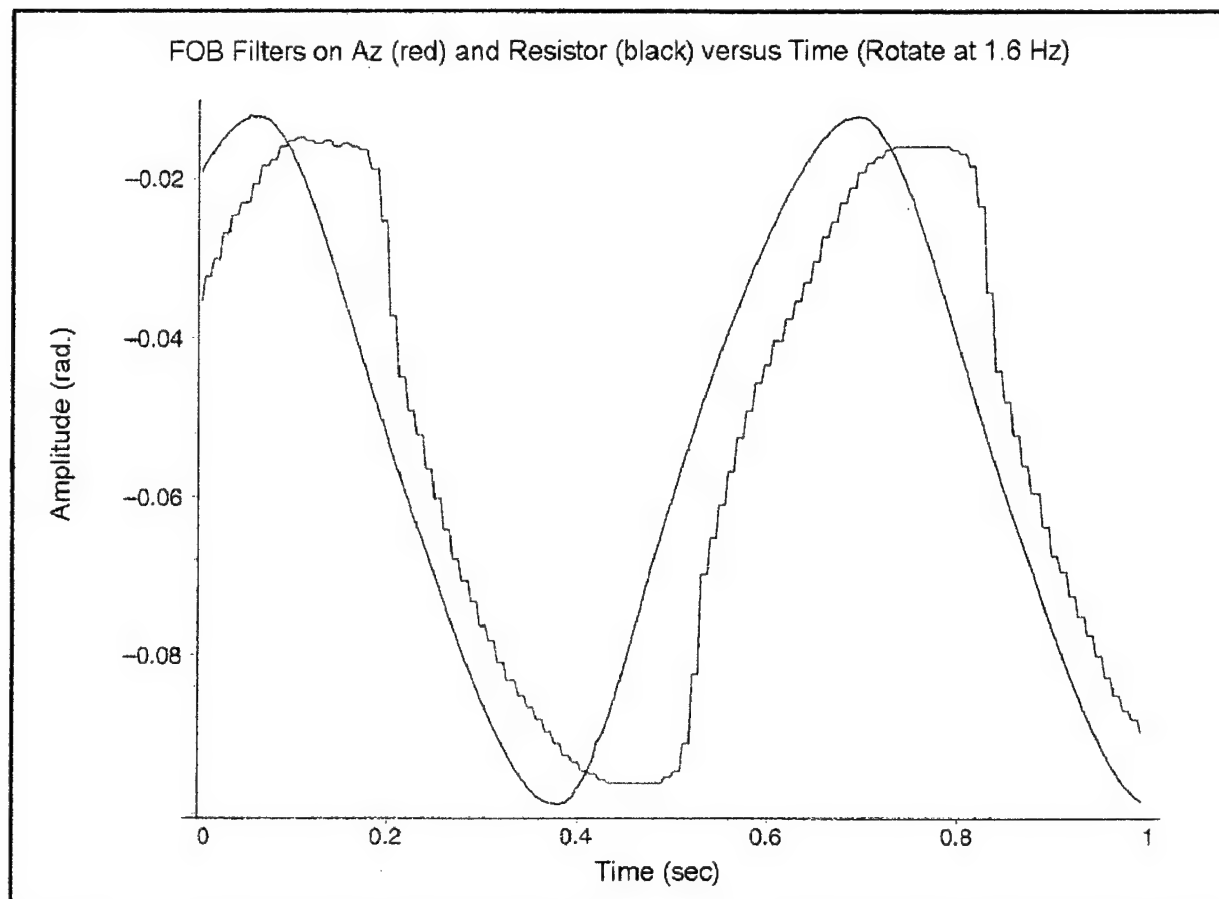

Figure B3.1
FOB (FILTERS ON) ROTATION VERSUS TIME

Description: The azimuth versus the analog sensor with sinusoidal rotation at two different frequencies. The loop slanted to the right (red) is at 1.6 Hz. The loop slanted to the left (blue) shows dramatic phase lag at 6.6 Hz.
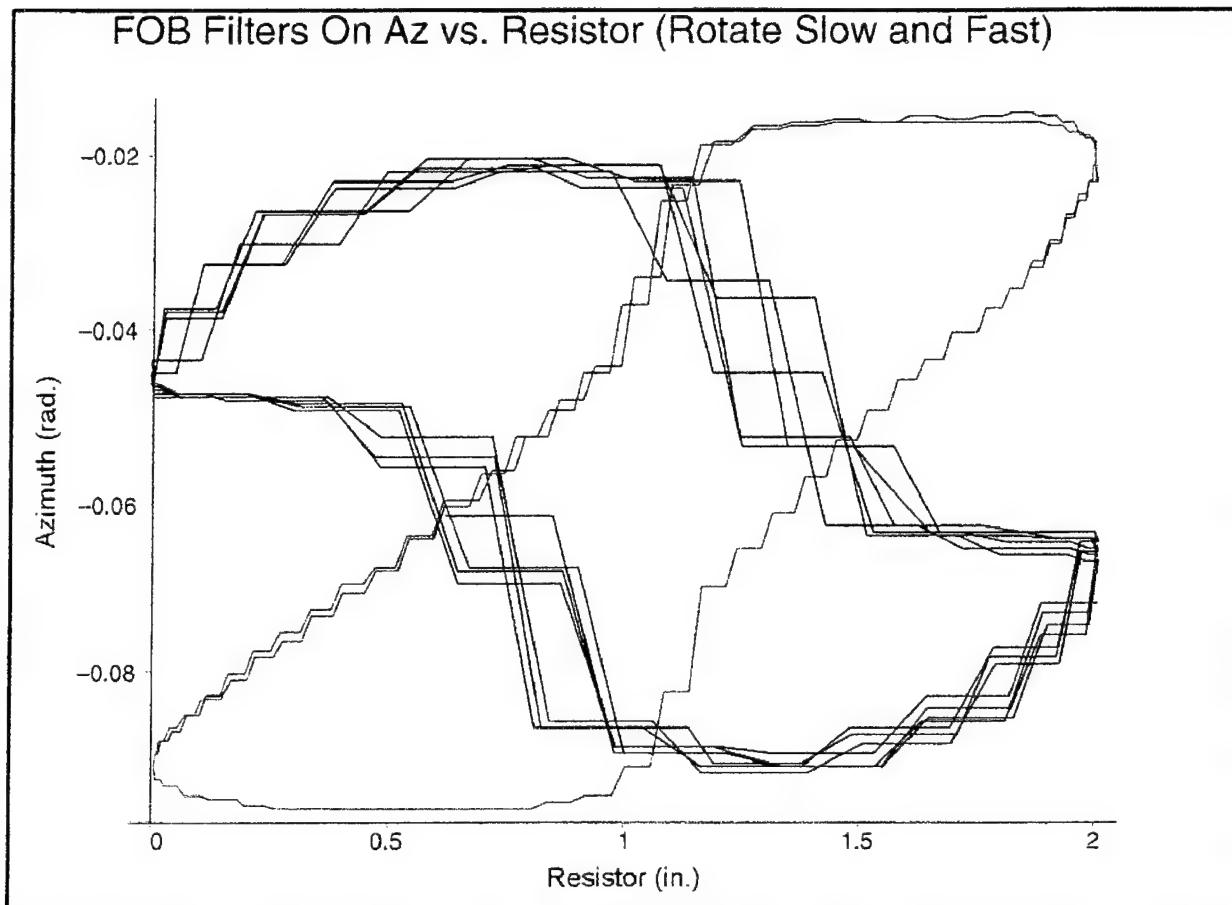

Figure B3.2
FOB (FILTERS ON) ROTATION VERSUS ANALOG SENSOR
(CHANGING FREQUENCY)

APPENDIX B

Description: The azimuth versus the analog sensor with sinusoidal rotation at two different transmitter locations. The transmitter was 8 in. from the receiver in the tall loop (red) and 27 in. from the receiver in the short loop (blue). The frequency is 1.6 Hz for both loops.
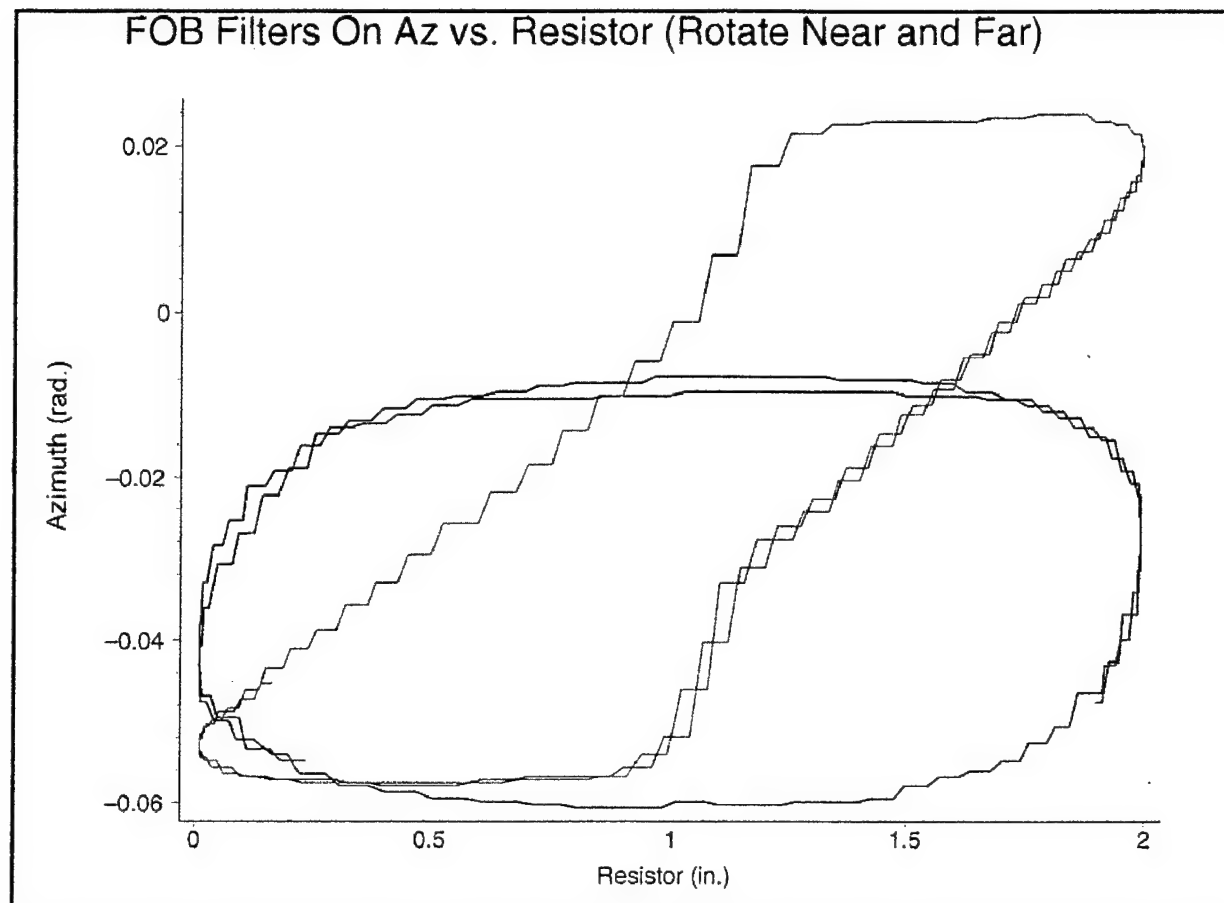

Figure B3.3
FOB (FILTERS ON) ROTATION VERSUS ANALOG SENSOR
(CHANGING LOCATION)

41   APPENDIX B

Description: The azimuth versus the Y axis as both parameters are stimulated in a sinusoidal motion. The thin loops indicate that there is almost no lag between the two parameters. The inner loop (red) is at 1.8 Hz and the outer loop (blue) is at 6.9 Hz.
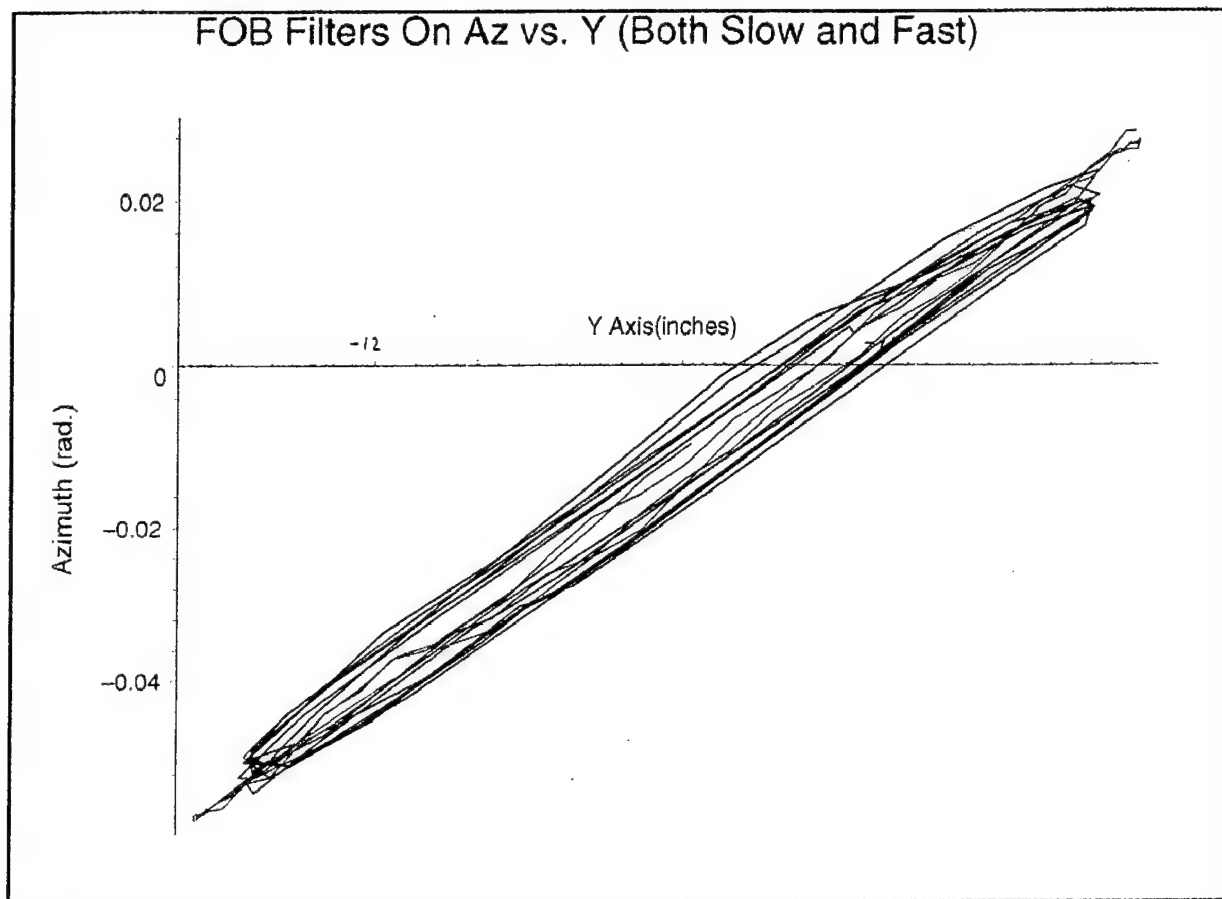

Figure B4.1
FOB (FILTERS ON) ROTATION VERSUS TRANSLATION
(CHANGING FREQUENCY)

Description: The azimuth versus the Y axis with the transmitter at different locations. The loops are thin near and far but they are noticeably fatter in the middle range.
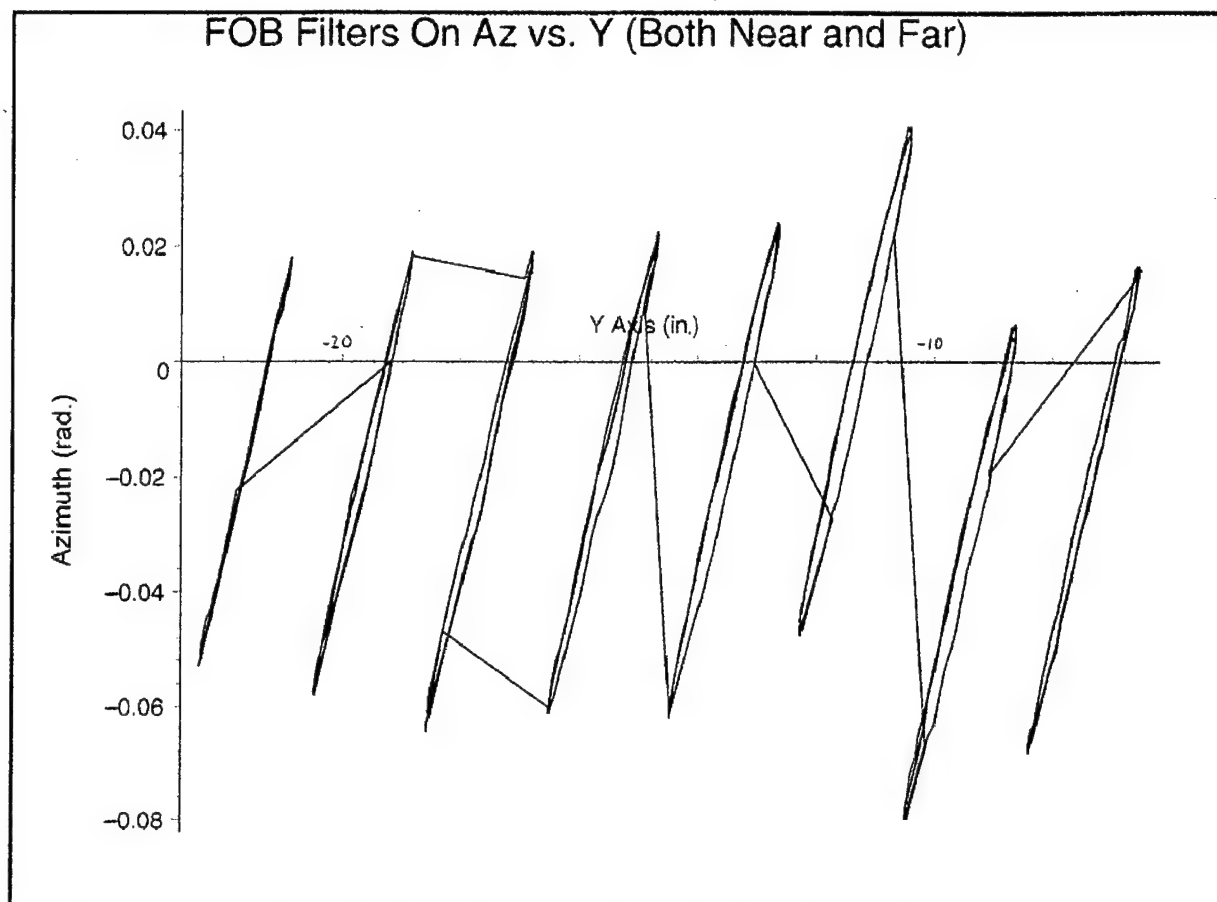

Figure B4.2
FOB (FILTERS ON) ROTATION VERSUS TRANSLATION
(CHANGING LOCATION)

THIS PAGE INTENTIONALLY LEFT BLANK

APPENDIX C
FLOCK OF BIRDS® TESTS (FILTERS OFF)

Configuration:
Single transmitter
Single receiver
316 samples per second (103 updates per second)

Note: The difference between sample rate and update rate results in a stair
step effect in the dynamic plots that should not be interpreted as noise.

Default filters off.
RS-232 connection at 38,400 baud.

C1 Static Test
Figure C1.1 FOB (filters off) Static Precision in Position
Figure C1.2 FOB (filters off) Static Precision in Orientation

C2 Dynamic Translation Test
Figure C2.1 FOB (filters off) Translation versus Time
Figure C2.2 FOB (filters off) Translation versus Analog Sensor (Changing Frequency)
Figure C2.3 FOB (filters off) Nonstimulated Parameter (Changing Frequency)
Figure C2.4 FOB (filters off) Translation versus Analog Sensor (Changing Location)
Figure C2.5 FOB (filters off) Nonstimulated Parameter(Changing Location)

C3 Dynamic Rotation Test
Figure C3.1 FOB (filters off) Rotation versus Time
Figure C3.2 FOB (filters off) Rotation versus Analog Sensor (Changing Frequency)
Figure C3.3 FOB (filters off) Rotation versus Analog Sensor (Changing Location)

C4 Dynamic Translation and Rotation Test
Figure C4.1 FOB (filters off) Rotation versus Translation (Changing Frequency)
Figure C4.2 FOB (filters off) Rotation versus Translation (Changing Location)

Description: The RMS of the noise in position parameters as a function of distance between the transmitter and the receiver as measured along the X axis by the tracker. Without the filters, the noise increases rapidly in all three position parameters X (red), Y (green), and Z (blue) as distance increases.
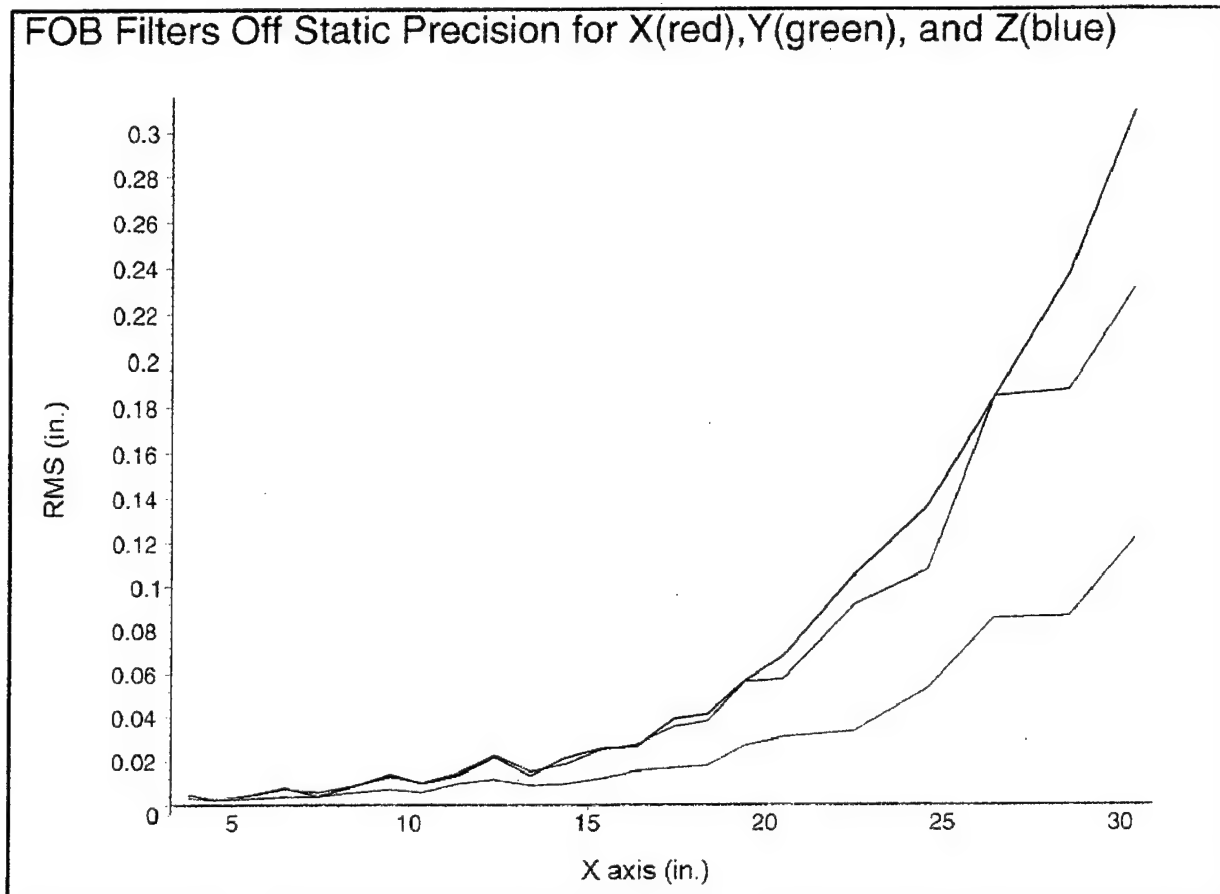

Figure C1.1
FOB (FILTERS OFF) STATIC PRECISION IN POSITION

DISTRIBUTION:

ASN RD&E (PEO(T))	(1)
ASN RD&A (PEO(A))	(1)
ASN RD&A (PEO(CU))	(1)
ASN RD&A (PEO(CU)CT))	(1)
ASN RD&A (PEO(CU)U)	(1)
ASN RD&A (PEO(CU)UD)	(1)
ASN RD&A (PEO(CU)UT)	(1)
ASN RD&A (PEO(CU)AQ)	(1)
ASN RD&A (PEO(T) (PMA-201))	(1)
ASN RD&A (PEO(T) (PMA-231))	(1)
ASN RD&A (PEO(T) (PMA-233))	(1)
ASN RD&A (PEO(T) (PMA-234))	(1)
ASN RD&A (PEO(T) (PMA-241))	(1)
ASN RD&A (PEO(T) (PMA-242))	(1)
ASN RD&A (PEO(T) (PMA-259))	(1)
ASN RD&A (PEO(T) (PMA-265))	(1)
ASN RD&A (PEO(T) (PMA-272))	(1)
ASN RD&A (PEO(A) (PMA-257))	(1)
ASN RD&A (PEO(A) (PMA-261))	(1)
ASN RD&A (PEO(A) (PMA-264))	(1)
ASN RD&A (PEO(A) (PMA-271))	(1)
ASN RD&A (PEO(A) (PMA-273))	(1)
ASN RD&A (PEO(A) (PMA-275))	(1)
ASN RD&A (PEO(A) (PMA-276))	(1)
ASN RD&A (PEO(A) (PMA-290))	(1)
ASN RD&A (PEO(A) (PMA-299))	(1)
ASN RD&A (PEO(CU) (PMA-263))	(1)
NAVAIRSYSCOM (PMA-200)	(1)
NAVAIRSYSCOM (PMA-202)	(10)
NAVAIRSYSCOM (PMA-205)	(10)
NAVAIRSYSCOM (PMA-209)	(1)
NAVAIRSYSCOM (PMA-213)	(1)
NAVAIRSYSCOM (PMJ01)	(1)
NAVAIRSYSCOM (AIR-1.0)	(1)
NAVAIRSYSCOM (AIR-2.0B)	(1)
NAVAIRSYSCOM (AIR-4.0)	(1)
NAVAIRSYSCOM (AIR-4.0A)	(1)
NAVAIRSYSCOM (AIR-4.0B)	(1)
NAVAIRSYSCOM (AIR-4.0C)	(1)
NAVAIRSYSCOM (AIR-4.0T)	(1)
NAVAIRSYSCOM (AIR-4.1)	(1)
NAVAIRSYSCOM (AIR-4.5)	(1)

NTIS	(1)
U.S. Army Natick RD&E Center (SSCNC-YBH), Natick, MA	(1)
Wright Laboratory (LW/AA), Wright-Patterson AFB, OH	(1)
Wright Laboratory (LW/FIGP-1), Wright-Patterson AFB, OH	(1)
Armstrong Laboratory (AL/DFTO), Brooks AFB, TX	(1)
Armstrong Laboratory (AL/CFHP), Wright-Patterson AFB, OH	(1)
ONR, Arlington, VA	(3)
NAVAIRWARCENACDIV, Lakehurst, NJ	(1)
NAVAIRWARCENTRASYSDIV Orlando, FL	(2)
NAVAIRWARCENWPNDIV China Lake, CA	(3)
NASA Ames Research Center, Moffett Field, CA	(2)
NASA Lewis Research Center, Cleveland, OH	(2)
NASA Langley Research Center, Langley, VA	(2)
JSC Space Center, Houston, TX	(2)
NASA Kennedy Space Center, Cape Canaveral, FL	(2)
NASA Marshall Space Flight Center, Huntsville, AL	(2)
NASA Washington, DC	(2)
NASA Scientific and Technical Information Facility, College Park, MD	(2)
U.S. Army Aeroflight Dynamics Directorate, Moffett Field, CA	(2)
U.S. Army Aeroflight Dynamics Directorate, Fort Eustis, VA	(2)
U.S. Army Research Institute Field Office, Fort Rucker, AL	(2)
DARPA Roslyn, VA	(2)
NAMI Pensacola, FL	(2)
NAMRL Pensacola, FL	(2)
Naval Biodynamics Research Laboratory, New Orleans, LA	(2)
Naval Post Graduate School, Monterey, CA	(2)
NRL Washington, DC	(2)
NV&EOL Fort Belvoir, VA	(2)
U.S. Army Structures Laboratory, Langley, VA	(2)
USAF Flight Test Center, Edwards AFB, CA	(2)
U.S. Army Aviation Center, Fort Rucker, AL	(2)
U.S. Army Human Engineering Research Laboratory, Aberdeen Proving Ground, MD	(2)
U.S. Army Research Office, Durham, NC	(2)
U.S. Army Walter Reed Army Institute, Washington, DC	(2)
Armed Forces Staff College, Norfolk, VA	(1)
Atlantic Intelligence Command, Norfolk, VA	(1)
Consolidated Navy Electronic Warfare School, Pensacola, FL	(1)
Expeditionary Warfare Training Group, Atlantic, Norfolk, VA	(1)
Fleet and Mine Warfare Training, Charleston, SC	(1)
Fleet Technical Support Center, Atlantic, Portsmouth, VA	(1)
Joint Intelligence Center Pacific, Pearl Harbor, HI	(1)
Joint Training Analysis and Simulation Center, Suffolk, VA	(1)
Joint Warfare Analysis Center, Dahlgren, VA	(1)
Librarian of the Navy, Washington, DC	(1)

Marine Corps Headquarters Judge Advocate Division, Washington, DC	(1)
Marine Corps Historical Center, Washington, DC	(1)
Marine Corps Intelligence Activity Detachment, Quantico, VA	(1)
Marine Corps Logistics Base, Albany GA	(1)
Marine Corps Research Center, Quantico, VA	(1)
Marine Corps Systems Command, Quantico, VA	(1)
Marine Corps Tactical Systems Support Activity, Camp Pendelton, CA	(1)
National Naval Medical Center, Bethesda, MD	(1)
Nautilus Memorial, Groton, CT	(1)
Naval Academy, Annapolis, MD	(1)
Naval Amphibious Base, Coronado, San Diego, CA	(1)
Naval Audit Service, Falls Church, VA	(1)
Naval Command, Control and Ocean Surveillance Center East Coast In-Service Engineering Division, Charleston Detachment, North Charleston, SC	(1)
Naval Command, Control and Ocean Surveillance Center East Coast In-Service Engineering Division, Norfolk Detachment, Portsmouth, VA	(1)
Naval Command, Control and Ocean Surveillance Center RDT&E Division, San Diego, CA	(1)
Naval Command, Control and Ocean Surveillance Center West Coast In-Service Engineering Division, San Diego, CA	(1)
Naval Computer and Telecommunications Station, Washington, DC	(1)
Naval Dental Research Institute, Great Lakes, IL	(1)
Naval Dental School, Bethesda, MD	(1)
Naval Education and Training Center, Newport, RI	(1)
Naval Education and Training Program Support Activity, Pensacola, FL	(1)
Naval Explosive Ordnance Disposal Technology Center, Indian Head, MD	(1)
Naval Facilities Engineering Center, Port Hueneme, CA	(1)
Naval Facilities Engineering Command, Atlantic Division, Norfolk, VA	(1)
Naval Facilities Engineering Command, Pacific Division, Pearl Harbor, HI	(1)
Naval Health Research Center, San Diego, CA	(1)
Naval Hospital, Pensacola, FL	(1)
Naval Hospital, Portsmouth, VA	(1)
Naval Hospital, San Diego, CA	(1)
Naval Hospital, Twenty-nine Palms, CA	(1)
Naval Medical Research Center, Bethesda, MD	(1)
Naval Medical Research Institute Toxicology Division, Wright Patterson AFB, OH	(1)
Naval Observatory, Washington, DC	(1)
Naval Oceanographic Office, Stennis Space Center, MS	(1)
Naval Research Laboratory, Washington, DC	(1)
Naval Research Laboratory, Atmospheric Division, Monterey, CA	(1)
Naval Research Laboratory Detachment, Stennis Space Center, MS	(1)
Naval Safety Center, Norfolk, VA	(1)
Naval School, Civil Engineers Corps Officers, Port Hueneme, CA	(1)
Naval School of Health Sciences, Bethesda, MD	(1)

Naval Sea Systems Command, Arlington, VA   (1)
Naval Submarine Medical Research Laboratory, Groton, CT   (1)
Naval Supply Corps School, Athens, GA   (1)
Naval Surface Warfare Center, Carderock Division, Bethesda, MD   (1)
Naval Surface Warfare Center, Carderock Division, Philadelphia Site, Philadelphia, PA (1)
Naval Surface Warfare Center, Carderock Division, UERD, Chesapeake, VA   (1)
Naval Surface Warfare Center, Crane Division, Crane, IN   (1)
Naval Surface Warfare Center, Crane Division, Louisville, KY   (1)
Naval Surface Warfare Center, Dahlgren Division, Dahlgren, VA   (1)
Naval Surface Warfare Center, Dahlgren Division, Panama City, FL   (1)
Naval Surface Warfare Center, Indian Head, MD   (1)
Naval Undersea Warfare Center, New London Detachment, New London, CT   (1)
Naval Undersea Warfare Center, Newport Division, Newport, RI   (2)
Naval War College, Newport, RI   (1)
Naval Warfare Assessment Center, Corona, CA   (1)
Navy Judge Advocate General, Alexandria, VA   (1)
Navy Personnel Research and Development Center, San Diego, CA   (1)
Navy Ship Parts Control Center, Mechanicsburg, PA   (1)
Norfolk Naval Shipyard, Portsmouth, VA   (1)
Office of Naval Intelligence, Washington, DC   (1)
NAVAIRSYSCOMDET Patuxent River, MD   (1)
NAVAIRWARCENACDIV Patuxent River, MD   (2)
NAVTESTWINGLANT Patuxent River, MD (55TW01A)   (1)
NAVAIRWARCENACDIV Patuxent River, MD (4.6.4.2)   (150)
NAVAIRWARCENACDIV Patuxent River, MD (4.11)   (1)
NAVAIRWARCENACDIV Patuxent River, MD (Technical Publishing Team)   (1)
DTIC   (1)